Türkiye Klinikleri Biyoistatistik Dergisi
Turkiye Klinikleri Journal of Biostatistics Turkiye Klinikleri J Biostat. 2024;16(1):16-37

ORIGINAL RESEARCH ORİJİNAL ARAŞTIRMA DOI: 10.5336/biostatic.2023-100247

A Methodological Research on Radiogenomics: Combining Radiomics and Genomics for Classification

Radyogenomik Üzerine Metodolojik Bir Araştırma: Sınıflamada Radyomiks ve Genomiksin Birleştirilerek Kullanılması

Merve KAŞIKCI[a], Erdal COŞGUN[b], Erdem KARABULUT[a]

[a]Hacettepe University Faculty of Medicine, Department of Biostatistics, Ankara, Türkiye
[b]Genomics Team, Microsoft Research, Redmond, WA, USA

ABSTRACT Objective: Radiogenomics investigates the use of radiomics and genomics features in clinical decision-making. The purpose of this study is to classify a clinical outcome by using radiomics and genomics features. The performances of different classification methods are compared and the effect of feature selection on classification performance is investigated. **Material and Methods:** Non-small cell lung cancer dataset from The Cancer Imaging Archive was used. The type of histology was selected as binary clinical outcome for classification. This dataset contains computed tomography images and RNA-sequence gene expressions. To standardize features, z scaling was applied to radiomics features and logarithmic transformation was applied to genomics features. Data was divided into 70% train set and 30% test set. Classification was carried out by modeling only radiomics features, only genomics features, and radiomics and genomics features together. Elastic net, random forest, support vector machines, and XGBoost algorithms were used for classification. Different feature selection approaches were explored to see the effect of feature selection on classification. Performance measures were calculated by using the test set. **Results:** The use of radiomics and genomics features improved the classification performance of random forest and XGBoost when feature selection was either not applied or when AUC was used for the feature selection method and elastic net when Recursive Feature Elimination was used for feature selection. **Conclusion:** Feature selection-based classification approach has a limited impact on model performance. Also, integration of two different data sources does not result in higher performance for every classification method.

Keywords: Digital imaging and communications in medicine; gene expression data; classification; feature selection

ÖZET Amaç: Radyogenomiks, klinik karar vermede görüntü ve genetik özelliklerin kullanımını araştıran bir alandır. Bu çalışmanın amacı, görüntü ve genetik özellikleri kullanarak klinik bir değişkeni sınıflamaktır. Farklı sınıflama yöntemlerinin performansları karşılaştırılmış ve özellik seçiminin sınıflama performansına etkisi incelenmiştir. **Gereç ve Yöntemler:** Kanser Görüntüleme Arşivi veri tabanından elde edilen küçük hücreli olmayan akciğer kanseri veri seti kullanılmıştır. Sınıflamada kullanılan sonuç değişkeni iki durumlu olan histolojinin türü değişkenidir. Bu veri seti bilgisayarlı tomografi görüntülerini ve RNA dizileme yönteminden elde edien gen ifadelerini içerir. Özellikleri standartlaştırmak için görüntü özelliklerine z dönüşümü, genetik özelliklere logaritmik dönüşüm uygulanmıştır. Veri seti %70 eğitim seti ve %30 test seti olmak üzere ikiye bölünmüştür. Sınıflama analizleri yalnızca görüntü özellikleri, yalnızca genetik özellikler ve görüntü ile genetik özellikler birlikte kullanılarak gerçekleştirilir. Sınıflama için "elastic net, rastgele orman, destek vektör makineleri ve XGBoost" algoritmaları kullanılmıştır. Değişken seçiminin sınıflama performansları üzerindeki etkisinin incelenmesi için farklı değişken seçimi yaklaşımları uygulanmıştır. Performans ölçüleri test seti kullanılarak hesaplanmıştır. **Bulgular:** Görüntü ve genetik özelliklerin birlikte kullanımı, değişken seçimi uygulanmadığında veya değişken seçimi yöntem olarak AUC kullanıldığında rastgele orman ve XGBoost algoritmalarının, özellik seçimi için özyinelemeli özellik seçimi kullanıldığında ise elastic net algoritmasının sınıflama performansını iyileştirmiştir. **Sonuç:** Değişken seçimine dayalı sınıflama yaklaşımlarının model performansı üzerinde etkisi sınırlı olmuştur. Ayrıca iki farklı veri kaynağının entegrasyonu her sınıflandırma yöntemi için daha yüksek performansla sonuçlanmamıştır.

Anahtar kelimeler: Tıpta dijital görüntüleme ve iletişim; gen ifade verisi; sınıflama; değişken seçimi

TO CITE THIS ARTICLE:
Kaşıkcı M, Coşgun E, Karabulut E. A methodological research on radiogenomics: Combining radiomics and genomics for classification. Turkiye Klinikleri J Biostat. 2024;16(1):16-37.

Correspondence: Merve KAŞIKCI
Hacettepe University Faculty of Medicine, Department of Biostatistics, Ankara, Türkiye
E-mail: mervekasikci@hacettepe.edu.tr

Peer review under responsibility of Turkiye Klinikleri Journal of Biostatistics.

Received: 09 Nov 2023 ***Received in revised form:*** 06 Dec 2023 ***Accepted:*** 07 Dec 2023 ***Available online:*** 04 Jan 2024

Medical imaging is an important tool for screening, diagnosis, and prognosis of the disease. The structures of medical images vary in terms of the type of image and the devices from which they are obtained. As a result of the need for a standard for producing, storing, displaying, sending, and receiving medical images, the Digital Imaging and Communications in Medicine (DICOM) format is developed.[1] Along with the image data, DICOM files also contain detailed information about the patient, image, and study. Medical image data in DICOM format is processed to produce radiomics features. These features can be categorized as tumor density, tumor shape, and tissue properties.[2]

Genetic data is another source in the research of disease mechanisms. By analyzing omic-type genetic data, diseases can be studied based on genes, transcripts, proteins, and metabolomes. The concept of omics is derived from the suffix "-omics", which is the suffix of fields such as genomics, transcriptomics, proteomics, metabolomics, and epigenomics. Through technological advances such as new generation sequencing, large amounts of data with high clarity can be accessed. As genetic data sources, expression datasets (gene, protein, etc.) from omics are often used. Variant calling factor datasets, which contain information on variants in the genome using DNA and RNA sequencing, are also preferred.

Radiomics features are associated with tumor phenotypes, whereas genomics features identify the underlying genetic and molecular composition of a tumor.[3] Recent developments in healthcare have made it possible to access different types of data for a disease of interest. Radiogenomics, the combination of the terminologies "radiology" and "genomics", focuses on using medical imaging and genetic data together for a more comprehensive analysis of disease mechanisms. Radiogenomics studies are based on the hypothesis that certain genetic changes cause tissue-level changes in radiomics features such as tissue shape and texture in radiological appearance.[4] Radiomics features refer to the extraction of a large number of features from medical images and focus on the imaging characteristics of a disease. The combination of radiomics and genomics features leads to more precise decision support systems. If clinical data is available in addition to medical image and genetic data, clinical features can also be combined with other features in radiogenomics.

Radiogenomics is a growing field of study, with more research being conducted over time as seen in Figure 1. Machine learning methods are often preferred by researchers in radiogenomics studies because of their capacity to process large amounts of data in a time-efficient manner. Machine learning algorithms are commonly used for classification, clustering, and regression tasks. In this study, we focus on classification in the field of radiogenomics. Radiomics and genomics features are extensively used data sources in classification studies. The purpose of classification may be to discriminate subjects for a particular disease or condition, to define the subtype of the disease, or to predict a clinical outcome. Also, there are classification studies aimed at predicting a genetic variable. In a great deal of radiogenomics research, radiomics data is used to classify genetic variables. Nero et al. used radiomics features extracted from ultrasound images to predict germline BRCA1/2 gene status in women with healthy ovaries.[5] Di Giannatale et al. aimed to classify the amplification of MYCN gene, Lasocki et al. investigated genotype prediction, and Prencipe et al. proposed a model for EGFR and KRAS mutation status by using radiomics features.[6-8]

In addition to these studies, predicting a clinical outcome by using radiomics and genomics features together is possible, as we focused on in our research. Guo et al. used radiogenomics features for the prediction of clinical phenotypes including pathological stage, lymph node metastasis, status of estrogen receptor, status of progesterone receptor, and status of human epidermal growth factor receptor 2.[3] They utilized magnetic resonance imaging images and genetic data of 91 breast cancer patients from The Cancer Genome Atlas and The Cancer Imaging Archive (TCIA) databases. Gallivanone et al. carried out a study to classify breast cancer subtypes using genetic biomarkers (miRNA) and radiomics imaging features.[9-11] Shboul and Iftekharuddin conducted a study on the classification of TP53 mutation status using radiomics, genomics, and radiogenomics features, respectively.[12] They used a dataset consisting of 105 lower-grade gliomas patients.

Trivizakis et al. used non-small cell lung cancer (NSCLC) dataset, which includes computed tomography (CT) and positron emission tomography CT images and RNA-seq gene expression data.[13,14]

They combined radiomics and transcriptomics features to obtain a set of features they call radiotranscriptomics to classify EGFR mutation status (wild-type or mutant), KRAS mutation status (wild-type or mutant), and histology subtypes (adenocarcinoma and squamous cell carcinoma). Murphy et al. worked on a study for the prediction of biochemical recurrence and metastatic disease occurrence in prostate cancer patients.[15] They used CT images and micro-array gene expressions of patients.

The approaches preferred for variable selection and classification vary among the studies in the literature. The aim of this study is to compare the performances of different classification methods in radiomics alone, genomics alone, and radiogenomics models. Additionally, analyses were performed with and without feature selection to investigate the effect of feature selection. The paper is organized as follows. First, we provide a real dataset implementation about histology subtype classification by using radiomics and genomics features. Second, we present the findings of our study. Third, we discuss our results and the results of similar studies in the literature. At last, we conclude with the conclusion and further research.

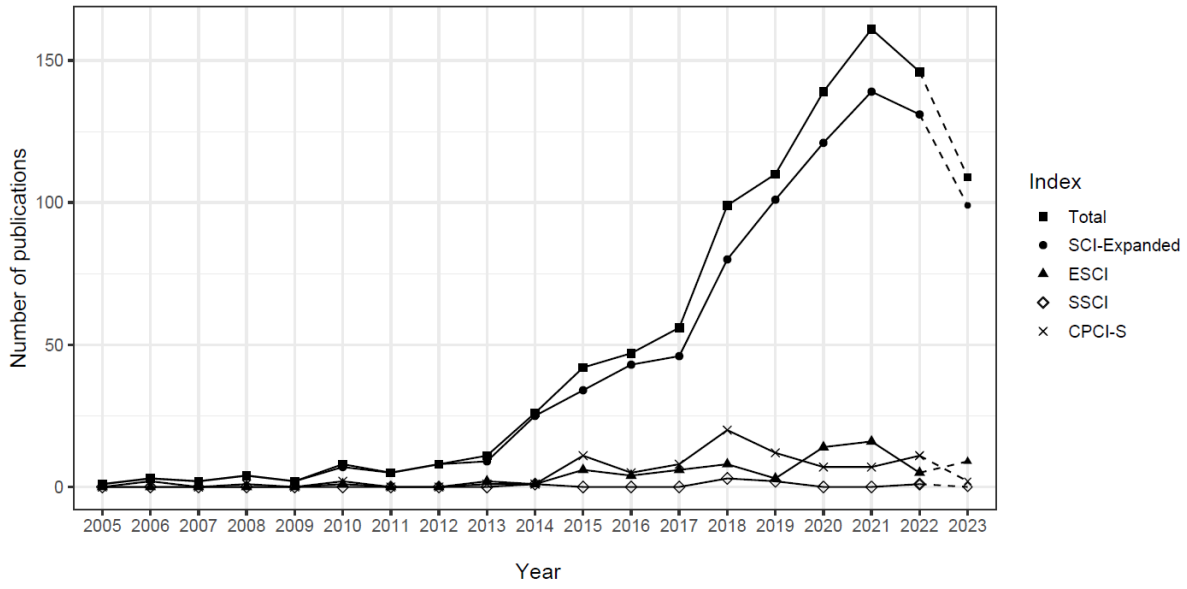

SCI-Expanded: Science Citation Index Expanded; ESCI: Emerging Sources Citation Index; SSCI: Social Sciences Citation Index; CPCI-S: Conference Proceedings Citation Index-Science.

FIGURE 1: The number of publications per year from Web of Science collection, including SCI-Expanded, ESCI, SSCI, and CPCI-S for articles on the topic of radiogenomics.

MATERIAL AND METHODS

DATASET

In this study, NSCLC dataset from the TCIA database was used.[10,14] The target variable for classification was selected as the histology type (adenocarcinoma and squamous cell carcinoma). This dataset contains CT images of 87 patients and RNA-seq gene expression dataset of 130 patients. Patients whose histology type is known and who have both image and genetic data were selected. As a result, the sample of the study consists of 58 patients.

DATA PRE-PROCESSING

Radiogenomics analysis pipeline notebook on GitHub was used to extract radiomics features directly from DICOM data.[16] Consequently, a total of 32 radiomics features were obtained, including 20 tumor density

features and 12 tumor shape features. The genomics features in the database were RNA-seq gene expression data normalized by Fragments Per Kilobase of transcript per Million mapped reads method. After eliminating genes with missing values, 5,268 genes were remaining. Radiomics and genomics features are generally distributed on a very wide scale. Therefore, z standardization was applied to radiomics features and logarithmic transformation was applied to genomics features.

METHODOLOGY

Following data pre-processing, the dataset was randomly partitioned into 70% train (n=40) and 30% (n=18) test sets. To investigate the effect of feature selection on classification, classification analyses were performed with and without feature selection. As feature selection methods, two approaches were considered. The first approach was a univariate method, in which Area Under the ROC Curve (AUC) was calculated for both image and genetic features. AUC values obtained from image features were observed to range from 0.501 to 0.668, while the AUC values obtained from genetic features were observed to range from 0.501 to 0.843 (Table 1 and Table 2 in Appendix). A common cut-off point was investigated for both sets of features, and this point was determined to be 0.60. As a result, features with AUC values greater than 0.60 were selected.

The second approach was recursive feature elimination (RFE) which is a random forest (RF)-based feature selection method. RFE method was chosen because it is an effective feature selection algorithm even when the input features are highly correlated.[17] The presence of highly correlated features, also known as multicollinearity, occurs especially in image data.

Elastic net regularized generalized linear models, RF, support vector machines (SVM) with diverse kernel functions (linear, radial basis, and polynomial), and XGBoost were performed on train set to obtain classification models. Since the small sample size, a separate validation set could not be used. During the training phase, 5-fold cross-validation and hyperparameter tuning were used to avoid classification algorithms from overfitting. tuneLength argument in the caret package was used to optimize hyperparameters.[18] tuneLength argument allows model hyperparameters to be tuned automatically.[19] Performance measures of classification methods, including accuracy, balanced accuracy, Matthew's correlation coefficient (MCC), sensitivity, specificity, positive predictive value (PPV), negative predictive value (NPV), and F1 score, were computed using the test set. caTools, caret, and GMDH2 R packages were used for obtaining AUC values, performing RFE and classification, calculating performance metrics, respectively.[18,20,21] The computation of performance measures are provided in Table 1.

TABLE 1: Calculations of performance measures.

Measure	Formula
Accuracy	$(\mathrm{TN}+\mathrm{TP})/(\mathrm{TP}+\mathrm{FN}+\mathrm{FP}+\mathrm{TN})$
Balanced accuracy	$(\mathrm{Sensitivity}+\mathrm{Specificity})/2$
MCC	$(\mathrm{TP}\times\mathrm{TN}+\mathrm{FP}\times\mathrm{FN})/\sqrt{(\mathrm{TP}+\mathrm{FP})(\mathrm{FN}+\mathrm{TN})(\mathrm{TP}+\mathrm{FN})(\mathrm{FP}+\mathrm{TN})}$
Sensitivity	$\mathrm{TP}/(\mathrm{TP}+\mathrm{FN})$
Specificity	$\mathrm{TN}/(\mathrm{TN}+\mathrm{FP})$
PPV	$\mathrm{TP}/(\mathrm{TP}+\mathrm{FP})$
NPV	$\mathrm{TN}/(\mathrm{TN}+\mathrm{FN})$
F1 score	$(2\times\mathrm{PPV}\times\mathrm{Sensitivity})/(\mathrm{PPV}+\mathrm{Sensitivity})$

MCC: Matthew's correlation coefficient; PPV: Positive predictive value; NPV: Negative predictive value; TP: True positive; TN: True negative; FP: False positive; FN: False negative.

RESULTS

In terms of histology type, adenocarcinoma accounts for 72% of the cases, whereas squamous cell carcinoma accounts for 28%. The class rate was kept when the dataset was separated into train and test sets. 29 of 40 patients in the train set and 13 of 18 patients in the test set had adenocarcinoma. Classification models were developed using the train set and model performances were assessed using the test set.

Table 2 shows the classification performances of models without feature selection. Accordingly, using radiomics and genomics features did not improve the classification performance of elastic net, SVM with linear kernel function, SVM with radial basis kernel function, and SVM with polynomial kernel function compared to using the radiomics or genomics features separately. For RF method, radiogenomics model provided an increase in almost all performance measures whereas for XGBoost method, balanced accuracy, specificity, PPV, and NPV were increased. In the results obtained from the combined use of radiomics and genomics variables, the increases in metrics, as compared to using either radiomics or genomics variables alone, are emphasized in bold in Table 2, Table 3, Table 4.

TABLE 2: Performance of classification algorithm on test set without feature selection.

	Accuracy	Balanced accuracy	MCC	Sensitivity	Specificity	PPV	NPV	F1 score
Elastic net-radiomics	0.667	0.462	-0.150	0.923	0.000	0.706	0.000	0.800
Elastic net-genomics	0.667	0.462	-0.150	0.923	0.000	0.706	0.000	0.800
Elastic net-radiogenomics	0.667	0.462	-0.150	0.923	0.000	0.706	0.000	0.800
RF-radiomics	0.667	0.523	0.055	0.846	0.200	0.733	0.333	0.786
RF-genomics	0.722	0.500	0.000	1.000	0.000	0.722	NA	0.839
RF-radiogenomics	0.778	0.600	0.391	1.000	0.200	0.765	1.000	0.867
SVM linear-radiomics	0.556	0.600	0.391	1.000	0.200	0.765	1.000	0.867
SVM linear-genomics	0.556	0.385	-0.277	0.769	0.000	0.667	0.000	0.714
SVM linear-radiogenomics	0.556	0.385	-0.277	0.769	0.000	0.667	0.000	0.714
SVM radial-radiomics	0.722	0.500	0.000	1.000	0.000	0.722	NA	0.839
SVM radial-genomics	0.722	0.500	0.000	1.000	0.000	0.722	NA	0.839
SVM radial-radiogenomics	0.722	0.500	0.000	1.000	0.000	0.722	NA	0.839
SVM poly-radiomics	0.722	0.500	0.000	1.000	0.000	0.722	NA	0.839
SVM poly-genomics	0.556	0.569	0.124	0.538	0.600	0.778	0.333	0.636
SVM poly-all	0.556	0.385	-0.277	0.769	0.000	0.667	0.000	0.714
XGBoost-radiomics	0.500	0.346	-0.331	0.692	0.000	0.643	0.000	0.667
XGBoost-genomics	0.667	0.462	-0.150	0.923	0.000	0.706	0.000	0.800
XGBoost-radiogenomics	0.667	0.523	0.055	0.846	0.200	0.733	0.333	0.786

RF: Random forest; SVM: Support vector machines; MCC: Matthew's correlation coefficient; PPV: Positive predictive value; NPV: Negative predictive value.

Classification performances with feature selection based on AUC values are provided in Table 3. The number of radiomics features with AUC values more than 0.60 was 11, while the number of genomics features was 1905. For XGBoost algorithm, radiogenomics model provided an increase in almost all performance measures whereas for RF, SVM with linear kernel function, and SVM with radial basis kernel function, balanced accuracy, specificity, and PPV were increased.

TABLE 3: Performance of classification algorithm on test set with feature selection based on AUC.

	Accuracy	Balanced accuracy	MCC	Sensitivity	Specificity	PPV	NPV	F1 score
Elastic net-radiomics	0.667	0.523	0.055	0.846	0.200	0.733	0.333	0.786
Elastic net-genomics	0.667	0.462	-0.150	0.923	0.000	0.706	0.000	0.800
Elastic net-radiogenomics	0.667	0.462	-0.150	0.923	0.000	0.706	0.000	0.800
RF-radiomics	0.556	0.446	-0.108	0.692	0.200	0.692	0.200	0.692
RF-genomics	0.722	0.500	NA	1.000	0.000	0.722	NA	0.839
RF-radiogenomics	0.722	0.562	0.175	0.923	0.200	0.750	0.500	0.828
SVM linear-radiomics	0.722	0.500	NA	1.000	0.000	0.722	NA	0.839
SVM linear-genomics	0.611	0.423	-0.219	0.846	0.000	0.688	0.000	0.759
SVM linear-radiogenomics	0.667	0.523	0.055	0.846	0.200	0.733	0.333	0.786
SVM radial-radiomics	0.722	0.500	NA	1.000	0.000	0.722	NA	0.839
SVM radial-genomics	0.722	0.500	NA	1.000	0.000	0.722	NA	0.839
SVM radial-radiogenomics	0.722	0.562	0.175	0.923	0.200	0.750	0.500	0.828
SVM poly-radiomics	0.722	0.500	NA	1.000	0.000	0.722	NA	0.839
SVM poly-genomics	0.611	0.423	-0.219	0.846	0.000	0.688	0.000	0.759
SVM poly-all	0.556	0.385	-0.277	0.769	0.000	0.667	0.000	0.714
XGBoost-radiomics	0.556	0.385	-0.277	0.769	0.000	0.667	0.000	0.714
XGBoost-genomics	0.556	0.385	-0.277	0.769	0.000	0.667	0.000	0.714
XGBoost-radiogenomics	0.778	0.723	0.446	0.846	0.600	0.846	0.600	0.846

RF: Random Forest; SVM: Support vector machines; MCC: Matthew's correlation coefficient; PPV: Positive predictive value; NPV: Negative predictive value.

Lastly, the importance of radiomics and genomics features was determined according to the RFE method. The top five most important features from both feature sets were chosen and classification models were developed using these features. According to the findings in Table 4, combining radiomics and genomics features provided an increase in almost all performance measures for elastic net method. For SVM with linear kernel function and SVM with radial basis kernel function, radiogenomics models have higher specificity comparing to radiomics and genomics models. On the other hand, modelling radiomics and genomics features together did not improve the classification performance of other methods.

TABLE 4: Performance of classification algorithm on test set with feature selection based on recursive feature elimination.

	Accuracy	Balanced accuracy	MCC	Sensitivity	Specificity	PPV	NPV	F1 score
Elastic net-radiomics	0.667	0.462	-0.150	0.923	0.000	0.706	0.000	0.800
Elastic net-genomics	0.667	0.523	0.055	0.846	0.200	0.733	0.333	0.786
Elastic net-radiogenomics	0.722	0.623	0.265	0.846	0.400	0.786	0.500	0.815
RF-radiomics	0.556	0.446	-0.108	0.692	0.200	0.692	0.200	0.692
RF-genomics	0.667	0.523	0.055	0.846	0.200	0.733	0.333	0.786
RF-radiogenomics	0.667	0.523	0.055	0.846	0.200	0.733	0.333	0.786
SVM linear-radiomics	0.722	0.500	0.000	1.000	0.000	0.722	NA	0.839
SVM linear-genomics	0.722	0.500	0.000	1.000	0.000	0.722	NA	0.839
SVM linear-radiogenomics	0.667	0.523	0.055	0.846	0.200	0.733	0.333	0.786
SVM radial-radiomics	0.722	0.500	0.000	1.000	0.000	0.722	NA	0.839
SVM radial-genomics	0.778	0.600	0.391	1.000	0.200	0.765	1.000	0.867
SVM radial-radiogenomics	0.611	0.546	0.088	0.692	0.400	0.750	0.333	0.720
SVM poly-radiomics	0.722	0.500	0.000	1.000	0.000	0.722	NA	0.839
SVM poly-genomics	0.722	0.562	0.175	0.923	0.200	0.750	0.500	0.828
SVM poly-all	0.611	0.423	-0.219	0.846	0.000	0.688	0.000	0.759
XGBoost-radiomics	0.556	0.446	-0.108	0.692	0.200	0.692	0.200	0.692
XGBoost-genomics	0.667	0.523	0.055	0.846	0.200	0.733	0.333	0.786
XGBoost-radiogenomics	0.611	0.485	-0.033	0.769	0.200	0.714	0.250	0.741

RF: Random forest; SVM: Support vector machines; MCC: Matthew's correlation coefficient; PPV: Positive predictive value; NPV: Negative predictive value.

DISCUSSION

Radiogenomics is a research area that investigates the integration and evaluation of different data sources. Using two separate data sources together, such as image and genetics, does not always result in greater performance than using them separately. According to our findings, radiogenomics models of XGBoost, elastic net, and RF methods had better classification performances than radiomics and genomics models depending on feature selection scenarios. However, there was no improvement in the classification model performances of other classification methods in radiogenomics models. Guo et al. reported that integrating radiomics and genomics datasets did not increase the classification performances in their study.[3] They stated that the reasons for the lack of improvement in terms of prediction in radiogenomics models could be the limited number of observations and the selected clinical outcomes. According to the study of Murphy et al., the accuracy of the genomic model in biochemical relapse classification and the radiomics model in MD classification was higher than the radiogenomics model.[15] In contrast, according to the studies of Gallivanone et al. and Shboul and Iftekharuddin radiogenomics models outperformed radiomics and genomics models in terms of classification.[11,12]

Radiogenomics requires the integration of multiple data sources. It could be difficult to access separate data sources for the same patients and this results in a limited number of observations. In addition to a small number of observations, as in our study, imbalanced class distributions are common in this field.[3,13,15] Considering the dataset used in this study is quite imbalanced in terms of histology type, specificity values of the models are often low. The test set contains 18 observations, 13 of which are adenocarcinomas and five of which are squamous cell carcinomas. When Table 2, Table 3, and Table 4 are evaluated together, it is seen that XGBoost method with radiogenomics model presented in Table 3 has the highest specificity. In these findings, three out of five squamous cell carcinoma observations in the test set were correctly identified. XGBoost method is built on a boosting algorithm, and because this algorithm assigns greater weight to misclassified observations, the model may exhibit high specificity even when dealing with imbalanced datasets.[22] The study's findings cannot be generalized because they are based on a single data set. As a result, the performance of XGBoost on imbalanced data requires further data and simulation studies.

Feature selection is one of the crucial factors in classification performance. The problem of high correlation between features may arise, especially for radiomics features. To handle this problem, Murhpy et al. selected features by filtering them based on their correlation with each other.[15] There are also studies that apply univariate approaches to reduce the number of features without considering correlations between features.[13,15] Methods such as LASSO and RFE, which select features by taking into account the relationships between variables, are also preferred by researchers.[3,12] In this study, we aim to investigate the effect of feature selection on classification. Therefore, we performed classification analysis without feature selection, with feature selection based on a univariate approach (AUC), and with feature selection based on an approach that considers the relationships between features (RFE). We wanted to explore how RFE would perform with a small number of important features, so we selected the five most important features from each dataset. RFE gives researchers the flexibility to select any number of important features. Among radiogenomics models, the highest F1 score is seen when RF method is used without feature selection and the highest balanced accuracy and MCC are seen when XGBoost is used with AUC based feature selection (Table 2, Table 3). Given the large number of feature selection techniques in the literature, this issue requires further investigation. Also, many different classification techniques can be used. Guo et al. used logistic regression with LASSO regularization, and Shboul and Iftekharuddin used RF.[3,12] Murphy et al. used also RF in their study.[15] Gallivanone et al. and Trivizakis et al. preferred to perform SVM.[11,13] Murphy et al. used logistic regression with LASSO regularization for the prediction of biochemical recurrence and RF for the prediction of metastatic disease occurrence. In common with these studies, we also preferred elastic net which is a form of regularized logistic regression, RF, and SVM. Additionally, we used SVM with different kernel functions and added XGBoost method.[15]

CONCLUSION

In this study, we focus on classification using radiomics and genomics features together. There is few research on this topic in the literature. Unlike other studies, this study aims to compare the classification performances of algorithms and investigate the effect of feature selection on classification. According to our findings, XGBoost, elastic net, and RF methods perform well in terms of classification with radiogenomics variables under different scenarios. Also, our study indicates that feature selection does not have much impact on classification performances. The findings of this study are not generalizable because they are based on a single data set. Since radiogenomics is based on the integration of different data sources, accessing radiogenomics data is quite difficult. We acknowledge that this is a preliminary study and as a future work, we are planning to conduct a comprehensive simulation study to increase the number of samples and features. With the help of the simulation study, the effects of classification algorithms and feature selection approaches on the combined evaluation of radiomics and genomics will be revealed more clearly.

Source of Finance

During this study, no financial or spiritual support was received neither from any pharmaceutical company that has a direct connection with the research subject, nor from a company that provides or produces medical instruments and materials which may negatively affect the evaluation process of this study.

Conflict of Interest

No conflicts of interest between the authors and/or family members of the scientific and medical committee members or members of the potential conflicts of interest, counseling, expertise, working conditions, share holding and similar situations in any firm.

Authorship Contributions

Idea/Concept: *Merve Kaşıkcı, Erdal Coşgun, Erdem Karabulut;* ***Design:*** *Merve Kaşıkcı, Erdal Coşgun, Erdem Karabulut;* ***Control/Supervision:*** *Erdem Karabulut, Erdal Coşgun;* ***Data Collection and/or Processing:*** *Merve Kaşıkcı;* ***Analysis and/or Interpretation:*** *Merve Kaşıkcı;* ***Literature Review:*** *Merve Kaşıkcı;* ***Writing the Article:*** *Merve Kaşıkcı.*

REFERENCES

1. Kamrani AK, Nasr EA. Rapid Prototyping: Theory and Practice. Vol. 6. 1st ed. New York: Springer Science & Business Media; 2006. [Crossref]
2. Giraud P, Giraud P, Gasnier A, El Ayachy R, Kreps S, Foy JP, et al. Radiomics and machine learning for radiotherapy in head and neck cancers. Front Oncol. 2019;9:174. [Crossref] [PubMed] [PMC]
3. Guo W, Li H, Zhu Y, Lan L, Yang S, Drukker K, et al; Tcga Breast Phenotype Research Group. Prediction of clinical phenotypes in invasive breast carcinomas from the integration of radiomics and genomics data. J Med Imaging (Bellingham). 2015;2(4):041007. [Crossref] [PubMed] [PMC]
4. Trivizakis E, Papadakis GZ, Souglakos I, Papanikolaou N, Koumakis L, Spandidos DA, et al. Artificial intelligence radiogenomics for advancing precision and effectiveness in oncologic care (Review). Int J Oncol. 2020;57(1):43-53. [Crossref] [PubMed] [PMC]
5. Nero C, Ciccarone F, Boldrini L, Lenkowicz J, Paris I, Capoluongo ED, et al. Germline BRCA 1-2 status prediction through ovarian ultrasound images radiogenomics: a hypothesis generating study (PROBE study). Sci Rep. 2020;10(1):16511. [Crossref] [PubMed] [PMC]
6. Di Giannatale A, Di Paolo PL, Curione D, Lenkowicz J, Napolitano A, Secinaro A, et al. Radiogenomics prediction for MYCN amplification in neuroblastoma: a hypothesis generating study. Pediatr Blood Cancer. 2021;68(9):e29110. [Crossref] [PubMed]
7. Lasocki A, Buckland ME, Drummond KJ, Wei H, Xie J, Christie M, et al. Conventional MRI features can predict the molecular subtype of adult grade 2-3 intracranial diffuse gliomas. Neuroradiology. 2022;64(12):2295-305. [Crossref] [PubMed] [PMC]
8. Prencipe B, Delprete C, Garolla E, Corallo F, Gravina M, Natalicchio MI, et al. An explainable radiogenomic framework to predict mutational status of KRAS and EGFR in lung adenocarcinoma patients. Bioengineering (Basel). 2023;10(7):747. [Crossref] [PubMed] [PMC]
9. National Cancer Institute [Internet]. The Cancer Genome Atlas Program (TCGA). Access date: [1 August 2023]. Access link: [Link]
10. National Cancer Institute [Internet]. © 2024 The Cancer Imaging Archive (TCIA) The Cancer Imaging Archive (TCIA). Access date: [1 August 2023]. Access link: [Link]
11. Gallivanone F, Cava C, Corsi F, Bertoli G, Castiglioni I. In Silico Approach for the definition of radiomirnomic signatures for breast cancer differential diagnosis. Int J Mol Sci. 2019;20(23):5825. [Crossref] [PubMed] [PMC]
12. Shboul ZA, Iftekharuddin KM. Efficacy of radiomics and genomics in predicting TP53 mutations in diffuse lower grade glioma. In: Krol A, Gimi BS, eds. Medical Imaging 2020: Biomedical Applications in Molecular, Structural, and Functional Imaging. Vol.11317. Houston, Texas, U.S.A: SPIE; 2020. p.238-44. [Crossref]
13. Trivizakis E, Souglakos J, Karantanas A, Marias K. Deep radiotranscriptomics of non-small cell lung carcinoma for assessing molecular and histology subtypes with a data-driven analysis. Diagnostics (Basel). 2021;11(12):2383. [Crossref] [PubMed] [PMC]
14. Bakr S, Gevaert O, Echegaray S, Ayers K, Zhou M, Shafiq M, et al. Data for NSCLC Radiogenomics (Version 4) [Data set]. The Cancer Imaging Archive. 2017. [Link]
15. Murphy R, Payan N, Osman S, Prise K, Hounsell A, O'Sullivan J, et al. PO-1769 Prostate cancer radiogenomics machine learning classification for predicting disease progression. Radiotherapy and Oncology. 2022;170:S1572-S1574 [Crossref]
16. Microsoft, genomicsnotebook [Internet]. RadioGenomics analysis pipeline. 2021. Access date: [15 August 2023]. Access link: [Link]
17. Gregorutti B, Michel B, Saint-Pierre P. Correlation and variable importance in random forests. Statistics and Computing. 2017;27:659-78. [Link] https://link.springer.com/article/10.1007/s11222-016-9646-1 [Crossref]
18. Kuhn M. caret: Classification and Regression Training. R package version 6.0-91. 2022. [Link]
19. Kuhn M, Wing J, Weston S, Williams A, Keefer C, Engelhardt A, et al. Package 'caret'. Package Manual. 2023. [Link]
20. Tuszynski J. caTools: Tools: Moving Window Statistics, GIF, Base64, ROC AUC, etc. R package version 1.18.2. 2021. [Link]
21. Dag O, Karabulut E, Alpar R. GMDH2: Binary Classification via GMDH-Type Neural Network Algorithms - R Package and Web-Based Tool. International Journal of Computational Intelligence Systems. 2019;12(2):649-60. [Crossref]
22. da Silva Neto SR, Tabosa Oliveira T, Teixeira IV, Aguiar de Oliveira SB, Souza Sampaio V, Lynn T, et al. Machine learning and deep learning techniques to support clinical diagnosis of arboviral diseases: a systematic review. PLoS Negl Trop Dis. 2022;16(1):e0010061. [Crossref] [PubMed] [PMC]

APPENDIX TABLE 1: AUC values for radiomics features (in descending order).

Variable	AUC	Variable	AUC	Variable	AUC	Variable	AUC	Variable	AUC	Variable	AUC	Variable	AUC	Variable	AUC
Elongation	0.668	SphericalDisprop	0.633	Max	0.577	Min	0.555	Ent	0.533	Uniformity	0.524	Engy	0.511	Interqualtile	0.505
Sphericity	0.633	90percent	0.597	Mean	0.577	Tol_Engy	0.545	SD	0.533	MinorAxisLen	0.524	MeshVol	0.511	rMAD	0.505
Compactness1	0.633	Flatness	0.580	Range	0.575	Skeness	0.545	Variance	0.533	Vol	0.520	Max3dDiameter	0.511	MajorAxisLen	0.505
Compactness2	0.633	Median	0.578	RMS	0.567	10percent	0.538	MAD	0.524	Surface	0.517	SurfaceVolRatio	0.508	Kurtosis	0.502

APPENDIX TABLE 2: AUC values for genomics features (in descending order).

Variable	AUC	Variable	AUC	Variable	AUC	Variable	AUC	Variable	AUC	Variable	AUC	Variable	AUC	Variable	AUC	Variable	AUC	Variable	AUC
ATP6V0A1	0.843	ZNF627	0.740	ELOVL5	0.715	HIVEP1	0.702	METAP2	0.693	AHI1	0.683	CREB3L2	0.677	CDC73	0.671	ZMIZ1	0.668	GATAD2A	0.661
CLSTN3	0.815	AFF4	0.737	GNB1	0.715	NISCH	0.702	RAB27A	0.693	B4GALT5	0.683	GRIPAP1	0.677	CLEC16A	0.671	ZNF217	0.668	GNE	0.661
RHEB	0.815	CCM2	0.737	GPCPD1	0.715	PCM1	0.702	RASGEF1B	0.693	CBFA2T2	0.683	LCMT1	0.677	CNOT4	0.671	ZSWIM6	0.668	HSDL2	0.661
C1orf27	0.809	LRP6	0.737	LOC202181	0.715	PPIL4	0.702	RNF145	0.693	CCDC132	0.683	LNX2	0.677	DDIT4	0.671	ACTR3	0.665	HUWE1	0.661
PLEKHG2	0.796	MYO6	0.737	MAN1A1	0.715	RNF144B	0.702	RPS6KB1	0.693	DSCR3	0.683	LUC7L3	0.677	DLGAP4	0.671	APOL1	0.665	ICA1	0.661
RGL1	0.796	PAPD7	0.737	NFATC3	0.715	RNF31	0.702	SF3A3	0.693	ELK4	0.683	MALAT1	0.677	ELF2	0.671	BRCC3	0.665	INTS12	0.661
RPF2	0.796	RAB7A	0.737	RAB2A	0.715	SLC37A3	0.702	STX3	0.693	FAM168A	0.683	MAN2A2	0.677	ESYT2	0.671	COG4	0.665	KIAA1958	0.661
LRRC37B	0.790	SETD3	0.737	RBL2	0.715	SLC39A8	0.702	TCP11L2	0.693	FAM177A1	0.683	MAP3K14	0.677	FIG4	0.671	COL5A1	0.665	KLHL7	0.661
BCL2L1	0.787	ZNF337	0.737	SYMPK	0.715	SRGAP2	0.702	TNS3	0.693	GCC2	0.683	MAX	0.677	GSPT1	0.671	CTCF	0.665	MCRS1	0.661
RAB2B	0.787	AARS	0.734	TAF13	0.715	TP53INP2	0.702	UBE2L3	0.693	HIVEP2	0.683	MKNK2	0.677	HDAC4	0.671	CYLD	0.665	MECP2	0.661
WWP1	0.787	LAMC1	0.734	TERF1	0.715	UBTD2	0.702	UTP18	0.693	KLHL20	0.683	MTF1	0.677	KANK1	0.671	ELOF1	0.665	OSBPL11	0.661
CUL1	0.781	NPC1	0.734	CCDC130	0.712	ZC3HAV1	0.702	WDR33	0.693	LOC100506710	0.683	NAGK	0.677	KDELR2	0.671	FNBP1	0.665	PAN3	0.661
FAM91A1	0.777	RARA	0.734	CLK3	0.712	AMBRA1	0.699	ADIPOR2	0.690	MKLN1	0.683	NGDN	0.677	KIAA0232	0.671	GATAD2B	0.665	PDHA1	0.661
MAST3	0.777	SCML1	0.734	DOPEY2	0.712	ATP6V1H	0.699	AGPAT3	0.690	PABPC1L	0.683	NUPR1	0.677	KLHL5	0.671	GORASP2	0.665	RASSF3	0.661
ZNF160	0.777	SLC23A2	0.734	FAM98A	0.712	CD55	0.699	BRE	0.690	RSRC2	0.683	PDXDC1	0.677	NAA50	0.671	HGSNAT	0.665	SLC7A6	0.661
DUSP10	0.774	SUDS3	0.734	METTL2B	0.712	ETV6	0.699	CCDC92	0.690	SLC2A1	0.683	PFKFB3	0.677	PPIP5K2	0.671	HLCS	0.665	SOCS6	0.661
OCRL	0.765	ZBED4	0.734	RALA	0.712	PITPNC1	0.699	CELSR1	0.690	SLC9A8	0.683	PPP2CA	0.677	RB1CC1	0.671	INPP4A	0.665	ST3GAL1	0.661
OGDH	0.765	GOSR2	0.730	SEC62	0.712	PRDM2	0.699	DCAF10	0.690	SMURF1	0.683	PSEN1	0.677	SCLT1	0.671	ITPKC	0.665	TFDP2	0.661
ZC3H7B	0.765	MEF2D	0.730	SETX	0.712	RPL37A	0.699	DDX60L	0.690	UBXN2B	0.683	RABL2B	0.677	SCYL3	0.671	MBIP	0.665	TFE3	0.661
ZNF274	0.765	MYLIP	0.730	SMAP1	0.712	SCFD1	0.699	DHX40	0.690	YPEL2	0.683	RAI14	0.677	SIPA1L3	0.671	MGMT	0.665	TOM1L1	0.661
IRF1	0.762	ZNF397	0.730	STRADA	0.712	SIK2	0.699	FBXW8	0.690	ADNP2	0.680	RSAD1	0.677	SMC6	0.671	MTG1	0.665	TP53INP1	0.661
ZNF780B	0.759	FAM83H	0.727	XPO6	0.712	TOX4	0.699	GPN2	0.690	ANKRD13A	0.680	SERPINB9	0.677	TMEM57	0.671	NEDD9	0.665	UBE2R2	0.661
CHMP4B	0.755	MBP	0.727	BRD4	0.708	ABCC9	0.696	GSDMB	0.690	ANKS1A	0.680	SMYD3	0.677	TOP1	0.671	NOB1	0.665	YTHDF3	0.661
DIAPH1	0.755	MKRN1	0.727	CDK10	0.708	ARHGEF3	0.696	IFT27	0.690	ARHGAP29	0.680	SOS2	0.677	TPR	0.671	NSL1	0.665	ZBTB41	0.661
ELMO2	0.755	OSGEP	0.727	CLK2	0.708	ASAP1	0.696	NLRC5	0.690	BCAS3	0.680	STAU1	0.677	WIPF2	0.671	PAPSS2	0.665	ZCCHC7	0.661
FMR1	0.755	TNFRSF21	0.727	EMB	0.708	CALCOCO2	0.696	PRKAG2	0.690	BRD1	0.680	USP3	0.677	ZNF529	0.671	PBXIP1	0.665	ZDHHC20	0.661
MTMR12	0.755	WDR37	0.727	FAM195B	0.708	DCP1A	0.696	PRPF38A	0.690	CHORDC1	0.680	XPC	0.677	ARRDC2	0.668	PPFIBP2	0.665	ZNF260	0.661
DDHD1	0.752	CDYL	0.724	FOXN3	0.708	GNA12	0.696	RALY	0.690	ELF1	0.680	ZNF264	0.677	ATP9A	0.668	PPP4R1	0.665	ZNFX1	0.661
GRAMD1A	0.752	CHD8	0.724	LGALS8	0.708	KDM2A	0.696	RNF138	0.690	ERC1	0.680	ATP11A	0.674	CHD3	0.668	PRPF38B	0.665	AKAP9	0.658

ITGA9	0.752	GOLPH3	0.724	PRPF4B	0.708	SMURF2	0.696	SDHAF2	0.690	FBXO38	0.680	CAB39	0.674	CMIP	0.668	PTP4A3	0.665	AMMECR1L	0.658
AHR	0.749	LMTK2	0.724	RANBP9	0.708	SNRNP35	0.696	SPOP	0.690	FEZ2	0.680	CLMN	0.674	CTSS	0.668	PTPN2	0.665	ANKRD52	0.658
B4GALT1	0.749	LRBA	0.724	SH2B3	0.708	STX17	0.696	STAT5B	0.690	FLNB	0.680	CRY1	0.674	DOCK4	0.668	RABIF	0.665	ATF6	0.658
EXOC4	0.749	MRC2	0.724	TAF4	0.708	TRIM4	0.696	STK24	0.690	FUT8	0.680	CTNNB1	0.674	DOCK8	0.668	RAD50	0.665	ATP5G2	0.658
RAB21	0.749	PHF20L1	0.724	ZSCAN29	0.708	VEZF1	0.696	TNKS	0.690	HEATR6	0.680	CYTH1	0.674	EDC4	0.668	SESTD1	0.665	B3GNT2	0.658
SEMA3C	0.749	DNAJC21	0.702	ARL15	0.677	CPEB4	0.661	IMP4	0.655	UBE2K	0.652	FEM1C	0.646	RABGAP1L	0.643	RNF114	0.639	TROVE2	0.636
TBC1D24	0.749	ERI3	0.702	ASAH1	0.677	DARS2	0.661	IMPACT	0.655	VAC14	0.652	FIP1L1	0.646	RANGAP1	0.643	RNF170	0.639	TTC39C	0.636
ANGEL2	0.746	WASL	0.696	C14orf159	0.677	DDI2	0.661	KDM4A	0.655	ACO2	0.649	FOXK2	0.646	RNF149	0.643	ROCK2	0.639	UAP1	0.636
PLAT	0.746	WDR20	0.696	C18orf25	0.677	DPM1	0.661	LHFPL2	0.655	ARHGEF11	0.649	GIGYF1	0.646	RPS6KA1	0.643	RPL4	0.639	UBA3	0.636
RPS6KA3	0.746	ANKRD13C	0.693	DCUN1D3	0.674	EXOC2	0.661	LITAF	0.655	ARMCX3	0.649	HERPUD2	0.646	SEMA4B	0.643	RRN3	0.639	UBE2G2	0.636
SPIRE1	0.746	AP3M2	0.693	ELP2	0.674	FNIP1	0.661	MPZL1	0.655	ATL2	0.649	IFNAR2	0.646	SLC35B3	0.643	RSF1	0.639	UBE4A	0.636
ZFAND6	0.746	BTF3L4	0.693	FBXO34	0.674	CDK5RAP2	0.658	MYH9	0.655	C16orf70	0.649	INPP5A	0.646	SMU1	0.643	SEC22B	0.639	USP53	0.636
ACSL4	0.743	CDK5RAP1	0.693	GALNT7	0.674	DDAH1	0.658	PAPD5	0.655	CAND1	0.649	ITPR1	0.646	SNHG5	0.643	SEC61A1	0.639	WDR19	0.636
ARNT	0.743	CLSTN1	0.693	GNAI3	0.674	EGFR	0.658	PIK3CB	0.655	CHCHD3	0.649	JAK2	0.646	SNX9	0.643	SOCS4	0.639	ZDHHC4	0.636
FKBP1A-SDCBP2	0.743	DAGLB	0.693	LPGAT1	0.674	ERICH1	0.658	PLIN2	0.655	CNTROB	0.649	JDP2	0.646	SPRED2	0.643	ST7	0.639	ZNF37BP	0.636
MLH3	0.743	DOCK11	0.693	PPP2R5E	0.674	FAM50A	0.658	PVRL2	0.655	CRTC3	0.649	LMBR1L	0.646	SRP54	0.643	STK38	0.639	ANAPC4	0.636
NOM1	0.743	EPB41	0.693	RABGEF1	0.674	FGFR1OP2	0.658	QKI	0.655	CXorf23	0.649	MAN1A2	0.646	SRPK1	0.643	TEP1	0.639	ANKIB1	0.636
PHACTR2	0.743	EPN2	0.693	RBM10	0.674	HTATSF1	0.658	SP110	0.655	DDX3X	0.649	MAP2K7	0.646	TCEB1	0.643	TES	0.639	CDC42SE2	0.636
RMND5B	0.743	FRMD4A	0.693	SEC14L1	0.674	INPP4B	0.658	SRPR	0.655	ENSA	0.649	METAP1	0.646	USP12	0.643	TMEM181	0.639	CES2	0.636
SAMD4A	0.743	GNA15	0.693	SETMAR	0.674	KIF13B	0.658	SRSF11	0.655	EPB41L5	0.649	NCALD	0.646	VDAC3	0.643	U2AF2	0.639	CLN5	0.636
ZCCHC2	0.743	HSBP1L1	0.693	SKAP2	0.674	LYST	0.658	TBC1D22B	0.655	FNBP1L	0.649	NCOA5	0.646	VPS45	0.643	USP28	0.639	CTDSP1	0.636
ASH1L	0.740	INTS1	0.693	SMCHD1	0.674	MED1	0.658	TMEM2	0.655	KLF6	0.649	PA2G4	0.646	VPS54	0.643	USP6NL	0.639	DCAF12	0.636
RAB11FIP3	0.740	INTS3	0.693	SNX27	0.674	MFHAS1	0.658	TSC22D1	0.655	KTN1	0.649	PACS1	0.646	VRK3	0.643	VPS37A	0.639	DRAM1	0.636
RAB1A	0.740	KBTBD2	0.693	VGLL4	0.674	MGAT5	0.658	TTC28	0.655	LARP4B	0.649	PACS2	0.646	XPO1	0.643	ZNF652	0.639	DYNLL2	0.636
STAT3	0.740	KIAA0319L	0.693	VPS41	0.674	MLLT1	0.658	UBL3	0.655	LPCAT3	0.649	PAPD4	0.646	ZNHIT6	0.643	ARHGDIA	0.639	ARHGEF2	0.633
WIPI2	0.724	KLHL21	0.693	ZMYND11	0.674	MPHOSPH9	0.658	VPS37B	0.655	LPXN	0.649	RAB28	0.646	ABHD5	0.639	ARIH1	0.639	ATMIN	0.633
ZFP36L2	0.724	KRR1	0.693	MAPKBP1	0.674	NDUFS1	0.658	VPS37C	0.655	MAGI1	0.649	RABGAP1	0.646	AKAP10	0.639	ATXN1	0.639	CALU	0.633
FMNL2	0.721	ATG7	0.687	ARMC8	0.671	NEK7	0.658	YEATS2	0.655	METTL17	0.649	SCAF8	0.646	ALS2	0.639	BAIAP2L1	0.639	CCDC6	0.633
GPRIN3	0.721	CLCC1	0.687	C11orf30	0.671	NOTCH1	0.658	ZNF516	0.655	NAPG	0.649	SEC23A	0.646	ARGLU1	0.639	EDEM1	0.636	CD99L2	0.633
LNPEP	0.721	CSPP1	0.687	FAM172A	0.668	NUDCD3	0.658	ZNF839	0.655	NCEH1	0.649	TET3	0.646	CDK5RAP3	0.639	ELP3	0.636	CEP170	0.633
RLIM	0.721	DPY19L3	0.687	MIF	0.668	PBX3	0.658	RALGAPB	0.655	NES	0.649	TNFAIP2	0.646	CDK8	0.639	EML4	0.636	CNOT3	0.633
TNRC18	0.721	FAM168B	0.687	MYADM	0.668	PELI1	0.658	SHB	0.655	PDE8A	0.649	TRAFD1	0.646	CHMP2B	0.639	EPS15	0.636	CXXC1	0.633
DNAJB6	0.718	GBAS	0.687	NGRN	0.668	PPARD	0.658	SLC30A1	0.655	PLXNA1	0.649	TSPYL2	0.646	DAPK3	0.639	ESCO1	0.636	DCTN4	0.633
FAM107B	0.718	GPBP1	0.687	NIPBL	0.668	PPWD1	0.658	SNF8	0.655	POLA1	0.649	UBA7	0.646	DCUN1D4	0.639	FBXW4	0.636	DDX58	0.633
GPR107	0.718	LIMD1	0.687	NOTCH2	0.668	PTPRM	0.658	ATXN7	0.652	REL	0.649	UBE2J2	0.646	DTD1	0.639	FYN	0.636	DYM	0.633
MBTD1	0.718	OGT	0.687	NRF1	0.668	RBM27	0.658	BRWD3	0.652	RNF213	0.649	UCP2	0.646	DUSP16	0.639	HACE1	0.636	DYNC1LI1	0.633
METRNL	0.718	PLEKHF2	0.687	PMM2	0.668	RFFL	0.658	C10orf76	0.652	RPL35A	0.649	USP14	0.646	EFR3A	0.639	HP1BP3	0.636	GALNT11	0.633
PIGG	0.718	RBM41	0.687	RGS5	0.668	RICTOR	0.658	COMMD1	0.652	RRBP1	0.649	VAPA	0.646	EXT2	0.639	HSPH1	0.636	KIAA0947	0.633
RALGDS	0.718	RNF216	0.687	RNF2	0.668	RPRD1A	0.658	CWC27	0.652	SENP2	0.649	ZHX2	0.646	FAM3A	0.639	IMMT	0.636	KIF1B	0.633

RASAL2	0.718	RNF24	0.687	RUFY1	0.668	SLC25A13	0.658	DTX3	0.652	SPTLC2	0.649	ZKSCAN5	0.646	FKBP15	0.639	KCTD2	0.636	LLPH	0.633
REV1	0.718	RUFY3	0.687	SIRT2	0.668	SLC44A1	0.658	FBXW11	0.652	STXBP5	0.649	ACCS	0.643	GPATCH8	0.639	KIAA0196	0.636	LOC150776	0.633
RFTN1	0.718	SLC35F5	0.687	SNX18	0.668	SNTB1	0.658	FUBP3	0.652	TBCK	0.649	AHCYL2	0.643	GRAMD3	0.639	LOC100133091	0.636	MALT1	0.633
ACBD3	0.715	SMYD4	0.687	STAU2	0.668	SNX2	0.658	FZD6	0.652	UBAP1	0.649	AMOTL1	0.643	GTPBP2	0.639	LRCH1	0.636	MEGF9	0.633
CRLS1	0.715	TAF1	0.687	TAF15	0.668	SRSF7	0.658	GNL3L	0.652	USP39	0.649	BACE2	0.643	HERC4	0.639	MICALL1	0.636	MYO1E	0.633
DAP	0.715	TJP2	0.687	TGFBR1	0.668	TAF2	0.658	HLTF	0.652	ZC3H7A	0.649	BICD2	0.643	KRI1	0.639	MPI	0.636	NCOA3	0.633
ARL8B	0.705	USP38	0.687	TOP2B	0.668	TM9SF4	0.658	KIFAP3	0.652	HDGFRP2	0.649	BNIP2	0.643	LACTB2	0.639	MSH3	0.636	NDUFV2	0.633
EHMT1	0.705	ZNF814	0.687	TTC8	0.668	TNPO3	0.658	KSR1	0.652	HEATR5A	0.649	CHURC1-FNTB	0.643	LEMD2	0.639	NBN	0.636	NR1D2	0.633
ENTPD4	0.705	HIPK2	0.680	UIMC1	0.668	VPS8	0.658	LOC646214	0.652	IP6K1	0.649	DNAJC1	0.643	LPIN2	0.639	NCOA6	0.636	NR3C1	0.633
EPAS1	0.705	IQCG	0.680	XRN2	0.668	ZDHHC3	0.658	MYO5A	0.652	KCTD9	0.649	ENC1	0.643	MARK3	0.639	NDEL1	0.636	NUP188	0.633
FERMT2	0.705	KIAA0226	0.680	SHOC2	0.665	ZDHHC9	0.658	NCOR2	0.652	AIFM1	0.646	FBXL17	0.643	NAV2	0.639	PANK3	0.636	PDCD5	0.633
KIAA0040	0.705	KIAA0586	0.680	SMG7	0.665	ZNF592	0.658	PTPRB	0.652	ARFGEF2	0.646	GGNBP2	0.643	NOL12	0.639	PBRM1	0.636	PEX2	0.633
LMBR1	0.705	LPIN3	0.680	SPRED1	0.665	ALCAM	0.655	RAPGEF5	0.652	ARSA	0.646	H2AFY	0.643	NPEPPS	0.639	PRKCE	0.636	PIGA	0.633
MKL1	0.705	MIS18BP1	0.680	STAG2	0.665	BACH1	0.655	SDHAP3	0.652	BCKDHB	0.646	HCFC1	0.643	NSMCE2	0.639	PTPN6	0.636	PTPRA	0.633
MPP5	0.705	MLLT4	0.680	SYTL1	0.665	BGN	0.655	SPPL3	0.652	CADPS2	0.646	IFNAR1	0.643	PCNX	0.639	RAB10	0.636	PTPRE	0.633
RBM47	0.705	PRRC2B	0.680	TMCO4	0.665	BMPR2	0.655	SS18	0.652	CCDC102B	0.646	IFRD1	0.643	PIK3C2B	0.639	RAB8A	0.636	RAB11FIP1	0.633
RPL37	0.705	PTPRJ	0.680	UBAP2L	0.665	DDX52	0.655	SUN1	0.652	CD24	0.646	KPNA5	0.643	PIK3C3	0.639	RNF38	0.636	RAB18	0.633
RPRD2	0.705	RNF19A	0.680	XRCC5	0.665	DLST	0.655	TAOK2	0.652	CGGBP1	0.646	MTHFD2	0.643	PIP4K2A	0.639	SESN1	0.636	RBM33	0.633
SSH3	0.705	TAB2	0.680	ACTR10	0.661	DYNC2H1	0.655	TMED5	0.652	CSRNP2	0.646	MTR	0.643	PLEKHA3	0.639	SOX4	0.636	RIF1	0.633
TRIM38	0.705	TMEM50B	0.680	ANKRD50	0.661	EDEM3	0.655	TRAPPC8	0.652	CTSA	0.646	MYH10	0.643	PODXL	0.639	STK40	0.636	RORA	0.633
ZFYVE1	0.705	XPR1	0.680	CCNY	0.661	EIF2AK4	0.655	TSC22D2	0.652	CUL3	0.646	NF1	0.643	PPIL2	0.639	TAF8	0.636	RPS6KC1	0.633
BLZF1	0.702	ZNF251	0.680	CCS	0.661	FAM63B	0.655	TTC3	0.652	DHX8	0.646	NGLY1	0.643	PRRC2C	0.639	TNK2	0.636	SAMD9L	0.633
COL5A2	0.702	ZNF507	0.680	CDC27	0.661	GOLGB1	0.655	TTF2	0.652	FAM63A	0.646	PHIP	0.643	RAB5A	0.639	TRIB1	0.636	SF3B3	0.633
CREB1	0.702	ANKH	0.677	CERK	0.661	HKR1	0.655	TTI1	0.652	FBXO25	0.646	PPP1R12B	0.643	RBM15	0.639	TRIP11	0.636	SLC25A16	0.633
SLC25A25	0.633	RAB11FIP4	0.630	KLF4	0.627	ERF	0.624	CKAP4	0.621	CBLB	0.618	TTC17	0.618	PPP1R12A	0.614	IL6ST	0.611	CHPF2	0.608
SNHG10	0.633	RC3H1	0.630	KPNA1	0.627	ERGIC1	0.624	DCLRE1C	0.621	CHID1	0.618	U2SURP	0.618	PPP2R3A	0.614	ITGA6	0.611	COL6A2	0.608
SORT1	0.633	RGS2	0.630	LEPRE1	0.627	FAM179B	0.624	EPS15L1	0.621	CNOT10	0.618	UBR5	0.618	PPP3CA	0.614	ITSN2	0.611	CTTNBP2NL	0.608
SP100	0.633	RHOBTB3	0.630	LEPROTL1	0.627	FEM1A	0.624	ESF1	0.621	DDX27	0.618	ZDHHC21	0.618	PREPL	0.614	LRRK2	0.611	DLG5	0.608
SREBF1	0.633	RLF	0.630	MAFK	0.627	FNDC3B	0.624	FASTKD2	0.621	DIP2A	0.618	ZNF33B	0.618	PVR	0.614	MAP2K4	0.611	DTX2	0.608
SYTL2	0.633	SBF2	0.630	MED13	0.627	HDAC5	0.624	FBXL3	0.621	DUSP23	0.618	AAK1	0.614	RAB31	0.614	MAP4K4	0.611	EPSTI1	0.608
TMEM167A	0.633	SDC1	0.630	MFSD6	0.627	HIPK3	0.624	FRK	0.621	ENG	0.618	ACP6	0.614	RANBP3	0.614	MAPKAPK2	0.611	ETV5	0.608
TRMT2B	0.633	SGMS1	0.630	MIPOL1	0.627	HIST1H4H	0.624	GPATCH2	0.621	EPHB4	0.618	AGFG1	0.614	RBM3	0.614	MED25	0.611	FOXO3	0.608
UBAC2	0.633	SLC39A11	0.630	N4BP1	0.627	HSD17B4	0.624	GRB2	0.621	ETNK1	0.618	ARF4	0.614	RSPH3	0.614	MORF4L2	0.611	GAS8	0.608
UBQLN1	0.633	SNHG6	0.630	NOD1	0.627	KCTD20	0.624	GTF2IRD1	0.621	FAM13A	0.618	ARFGAP1	0.614	RXRA	0.614	MTHFR	0.611	GLCCI1	0.608
UHRF1BP1L	0.633	SNX6	0.630	NT5DC1	0.627	KDM6B	0.624	HEBP1	0.621	FAM160A2	0.618	ARID2	0.614	SAP30BP	0.614	NFKB1	0.611	GLE1	0.608
UPF2	0.633	SRCAP	0.630	NUB1	0.627	L3MBTL2	0.624	IP6K2	0.621	FAM188A	0.618	ATP13A3	0.614	SLC12A2	0.614	NHP2L1	0.611	GNAQ	0.608
USP11	0.633	SUPT7L	0.630	POLE	0.627	LAMP2	0.624	IPO9	0.621	FER	0.618	B2M	0.614	SLC39A10	0.614	NNT	0.611	GTF3C4	0.608
UTP23	0.633	SYNE1	0.630	PPP2CB	0.627	MAP4K5	0.624	IQSEC1	0.621	FLAD1	0.618	CCL2	0.614	SLC39A9	0.614	OTUD1	0.611	HEBP2	0.608
WIPF1	0.633	TAPT1	0.630	PSIP1	0.627	MCCC1	0.624	JMJD1C	0.621	GFM1	0.618	CHST11	0.614	SMC5	0.614	OTUD5	0.611	HELZ	0.608

YTHDC2	0.633	THOC2	0.630	PUS7L	0.627	MED17	0.624	KARS	0.621	HDGFRP3	0.618	CLINT1	0.614	SPSB1	0.614	PAK1	0.611	HERC1	0.608
ZNF10	0.633	TSG101	0.630	QSOX1	0.627	MIER3	0.624	KRIT1	0.621	HEXB	0.618	CNPY3	0.614	TATDN1	0.614	PES1	0.611	LGALS3	0.608
ZNF862	0.633	USP25	0.630	RAP2A	0.627	MTRR	0.624	LRRC8B	0.621	HIRA	0.618	COL6A1	0.614	TMEM39A	0.614	PIBF1	0.611	LRIG1	0.608
ACER3	0.630	VCPIP1	0.630	RCAN1	0.627	NCOA1	0.624	MAPK1IP1L	0.621	IGFBP4	0.618	DENND4A	0.614	UBE2H	0.614	PIP4K2B	0.611	LRRC40	0.608
GOLT1B	0.633	YME1L1	0.630	RCOR3	0.627	OSBPL3	0.624	METTL15	0.621	ITPK1	0.618	DIP2B	0.614	VAPB	0.614	POU2F1	0.611	LRRC58	0.608
GPR125	0.633	ZNF623	0.630	RFWD2	0.627	PAFAH1B1	0.624	MIDN	0.621	ITSN1	0.618	DNAJC7	0.614	WAC	0.614	PPP2R5C	0.611	MCTP2	0.608
HIST2H2BF	0.633	ZNF708	0.630	RNMT	0.627	PDE12	0.624	MRPS21	0.621	KIAA0141	0.618	DTX4	0.614	WSB1	0.614	PPRC1	0.611	MIB1	0.608
ID2	0.633	ACSS2	0.627	SCMH1	0.627	PIGN	0.624	NAMPT	0.621	KIAA1432	0.618	ELK3	0.614	ZNF12	0.614	PTBP1	0.611	MRPL33	0.608
ANTXR1	0.630	ADCY6	0.627	SCYL2	0.627	PKP4	0.624	NCOA2	0.621	LMF2	0.618	ENAH	0.614	ZNF124	0.614	PTPRF	0.611	MRPL40	0.608
ATF7IP	0.630	AEBP1	0.627	SH3PXD2B	0.627	PPP1R12C	0.624	NDRG3	0.621	LPCAT1	0.618	ENOSF1	0.614	ZNF146	0.614	RBM7	0.611	MTHFD1	0.608
BRAF	0.630	AEBP2	0.627	SLC25A43	0.627	PPP3R1	0.624	NEK9	0.621	LRRFIP2	0.618	EPS8L2	0.614	AFTPH	0.611	RIPK1	0.611	MTMR3	0.608
CBX4	0.630	ANXA11	0.627	SNX13	0.627	PUS7	0.624	OCIAD1	0.621	MAP3K3	0.618	EXOC6	0.614	ANKRD12	0.611	RNF130	0.611	MTMR4	0.608
CENPB	0.630	AP2M1	0.627	SRSF5	0.627	QSER1	0.624	OXSR1	0.621	MAPRE2	0.618	FCF1	0.614	ANO6	0.611	RPL13	0.611	NDUFA5	0.608
CEP70	0.630	ARHGAP21	0.627	STK39	0.627	RHOT1	0.624	PARP14	0.621	NAP1L1	0.618	FUCA1	0.614	ANXA4	0.611	S100A4	0.611	NFS1	0.608
CHD1	0.630	ARHGAP31	0.627	STRBP	0.627	RYBP	0.624	PGGT1B	0.621	NDFIP1	0.618	GABARAPL1	0.614	ARHGAP17	0.611	SAMM50	0.611	NIPAL3	0.608
CTBP2	0.630	ARHGAP5	0.627	SUPT6H	0.627	SAMD4B	0.624	PLEK	0.621	NDUFAF2	0.618	GNPTAB	0.614	ARPC5	0.611	SENP5	0.611	NRIP1	0.608
DAPK1	0.630	ATP10D	0.627	TMEM140	0.627	SH2D4A	0.624	POM121C	0.621	NEK4	0.618	HIPK1	0.614	ATRN	0.611	SH3RF1	0.611	NUP133	0.608
DHX9	0.630	ATP13A1	0.627	TNKS2	0.627	SLC35E1	0.624	RPS16	0.621	NOC2L	0.618	HNRNPA0	0.614	B3GALNT2	0.611	SNTB2	0.611	PANK2	0.608
FAM102A	0.630	ATP2B4	0.627	UBE2W	0.627	SLMAP	0.624	SLC4A7	0.621	PAFAH1B2	0.618	HSPB1	0.614	BBS9	0.611	SNX25	0.611	PDZD8	0.608
FLCN	0.630	ATP6AP2	0.627	WDR44	0.627	SNORA49	0.624	SMG1	0.621	PDE4DIP	0.618	INSIG1	0.614	C5orf22	0.611	SON	0.611	PMM1	0.608
FTO	0.630	BRWD1	0.627	WDR77	0.627	SSH2	0.624	STAT1	0.621	PITRM1	0.618	ITPR2	0.614	C5orf51	0.611	SPATS2L	0.611	POLR2D	0.608
GGA3	0.630	BZW2	0.627	YIPF6	0.627	STX18	0.624	STX6	0.621	PLCG2	0.618	KIAA1429	0.614	CD163	0.611	STX5	0.611	PRKACB	0.608
GPD1L	0.630	C1GALT1	0.627	ZDHHC2	0.627	TANK	0.624	SYNRG	0.621	PRKCH	0.618	KIAA2026	0.614	CEP192	0.611	TBC1D2B	0.611	PYGL	0.608
HMG20B	0.630	CD97	0.627	ZFP90	0.627	TMEM106B	0.624	TAF7	0.621	PSMA6	0.618	KLHL12	0.614	CHD2	0.611	TNPO2	0.611	RASSF4	0.608
KLHL28	0.630	CDC37	0.627	ZNF710	0.627	TSEN15	0.624	TCF12	0.621	PSMD7	0.618	LETM1	0.614	COG6	0.611	TTYH3	0.611	RPL34	0.608
LAP3	0.630	CEP350	0.627	ADAR	0.624	TSHZ1	0.624	TGFBI	0.621	ROCK1	0.618	MAP2K2	0.614	CSNK1D	0.611	USP9X	0.611	RPS24	0.608
MCMBP	0.630	CIR1	0.627	AKAP13	0.624	UBE2B	0.624	TGM2	0.621	RPP14	0.618	MAP2K3	0.614	CYB5A	0.611	WAPAL	0.611	SEC24D	0.608
MICAL2	0.630	CLPX	0.627	ANKHD1-EIF4EBP3	0.624	UBE2E2	0.624	TNFRSF10B	0.621	S100A16	0.618	MARK2	0.614	DHTKD1	0.611	WDR35	0.611	SEL1L	0.608
MOB2	0.630	COG5	0.627	AP3S1	0.624	UBLCP1	0.624	TRMT11	0.621	SGMS2	0.618	MBNL1	0.614	DNAJA3	0.611	ZBTB37	0.611	SHKBP1	0.608
MPRIP	0.630	COL1A2	0.627	ARHGAP26	0.624	UBN2	0.624	TUBGCP6	0.621	SH3BGRL	0.618	MCCC2	0.614	DOCK9	0.611	ZC3H13	0.611	SLC39A13	0.608
MRPL50	0.630	CYBB	0.627	ATF7	0.624	USP36	0.624	XBP1	0.621	SIPA1L1	0.618	MLKL	0.614	EIF2S1	0.611	ZC3H4	0.611	SLC41A1	0.608
NAA40	0.630	DEPDC5	0.627	ATXN2L	0.624	WDR11	0.624	XPO5	0.621	SLC39A6	0.618	MRPS5	0.614	EIF3A	0.611	ZNF506	0.611	SMARCE1	0.608
NAB1	0.630	DOCK5	0.627	BMPR1A	0.624	XIAP	0.624	ZBTB20	0.621	SLC9A3R1	0.618	NCKIPSD	0.614	EXOC5	0.611	ACAP2	0.608	SNX14	0.608
PAPOLA	0.630	DPY19L1	0.627	BTBD9	0.624	ZFAND3	0.624	ZNF148	0.621	SMEK2	0.618	NEDD4L	0.614	EZH1	0.611	ACO1	0.608	SNX30	0.608
PDE4D	0.630	ETF1	0.627	CDK17	0.624	AKAP8	0.621	ZNF3	0.621	SRBD1	0.618	NOLC1	0.614	FAF2	0.611	ACVR1B	0.608	SRP19	0.608
PDXK	0.630	EWSR1	0.627	CELF1	0.624	ALDH1A3	0.621	ZNF362	0.621	SRSF1	0.618	NPHP3-ACAD11	0.614	FAM192A	0.611	AGTPBP1	0.608	ST14	0.608
PI4K2A	0.630	FEM1B	0.627	CTDSPL2	0.624	ARHGAP12	0.621	AMZ2	0.618	STT3B	0.618	NSMAF	0.614	FAM193A	0.611	ANKRA2	0.608	STEAP4	0.608
PIAS2	0.630	FOSL2	0.627	CUX1	0.624	ARMC1	0.621	ASPSCR1	0.618	SURF6	0.618	NSUN2	0.614	FAM20B	0.611	ASH2L	0.608	STK3	0.608
PLEKHA2	0.630	FOXO1	0.627	CXorf40B	0.624	ATF3	0.621	ATIC	0.618	TAX1BP1	0.618	NUP214	0.614	FBXO28	0.611	BRF1	0.608	TBC1D9	0.608

PNPLA6	0.630	GPR116	0.627	DENND1B	0.624	BPGM	0.621	ATP6AP1	0.618	TLE3	0.618	NUS1	0.614	FBXO3	0.611	BTRC	0.608	TCEAL4	0.608
POLDIP3	0.630	H6PD	0.627	DLC1	0.624	CBFB	0.621	ATP6V1B2	0.618	TOP3B	0.618	PALLD	0.614	GIGYF2	0.611	CARHSP1	0.608	THRAP3	0.608
PPP6R2	0.630	ICAM1	0.627	DPY19L1P1	0.624	CDKN1B	0.621	BRI3	0.618	TRAF3	0.618	PARP4	0.614	HOPX	0.611	CCND3	0.608	TOM1	0.608
PRR14L	0.630	IRF3	0.627	EPC1	0.624	CHD6	0.621	C11orf54	0.618	TSPAN13	0.618	PPM1A	0.614	IKZF2	0.611	CEP290	0.608	TP53BP2	0.608
TSNARE1	0.608	PICK1	0.605	HDAC7	0.602	ATP6V1C1	0.599	RAPGEF1	0.599	ISG20L2	0.596	ARIH2	0.592	SLC3A2	0.592	HS2ST1	0.589	ACACA	0.586
VDAC2	0.608	PNPLA8	0.605	HIST1H2AG	0.602	BCAS2	0.599	RPS6KA2	0.599	ITFG1	0.596	ARL5B	0.592	SMAD1	0.592	ILKAP	0.589	ACVR1	0.586
VPS11	0.608	POLR2E	0.605	IKBKB	0.602	BRPF3	0.599	SAP130	0.599	JARID2	0.596	ARL6IP5	0.592	SPINT1	0.592	JAK1	0.589	ANP32E	0.586
XPO7	0.608	POSTN	0.605	IRAK1	0.602	C12orf49	0.599	SAR1B	0.599	KAT2B	0.596	ASB6	0.592	SSBP3	0.592	KIAA0355	0.589	AP2B1	0.586
XRCC1	0.608	PSMD11	0.605	ITCH	0.602	C1orf198	0.599	SCAF11	0.599	KIF3A	0.596	ATXN1L	0.592	ST13	0.592	KIAA2013	0.589	AP3B1	0.586
ZBTB7A	0.608	PTPN12	0.605	ITGA3	0.602	C5orf42	0.599	SCAF4	0.599	LDLR	0.596	BBS2	0.592	STX12	0.592	LOC100131564	0.589	BRMS1	0.586
ZFP36L1	0.608	RAP1A	0.605	KIF3B	0.602	CASD1	0.599	SEC13	0.599	LRIG2	0.596	BOD1	0.592	STYX	0.592	LTBP3	0.589	CARKD	0.586
ZNF236	0.608	RBMS1	0.605	KLHDC10	0.602	CD276	0.599	SERPINH1	0.599	LYSMD3	0.596	BTBD7	0.592	TAB3	0.592	LYPLA1	0.589	CBX3	0.586
ZZEF1	0.608	RBMS2	0.605	LETMD1	0.602	CDK13	0.599	SH3D19	0.599	MAPK9	0.596	C5orf15	0.592	TGFBR2	0.592	MAP2K1	0.589	CDKN1A	0.586
ABL2	0.605	RERE	0.605	LOC146880	0.602	CHIC2	0.599	SNRPA1	0.599	MEMO1	0.596	CDC42SE1	0.592	TNRC6A	0.592	MDK	0.589	CDS2	0.586
APOE	0.605	RPL19	0.605	LYN	0.602	CITED2	0.599	SPTBN1	0.599	MMGT1	0.596	CDKL5	0.592	TYW1	0.592	MRPS30	0.589	CUL4B	0.586
ARFGEF1	0.605	RYK	0.605	NAA15	0.602	CPD	0.599	STK10	0.599	MYO9A	0.596	CLASP2	0.592	UBE2Q2	0.592	MSI2	0.589	CXCR4	0.586
ARRB2	0.605	SEC22A	0.605	NHSL1	0.602	DCAF5	0.599	TFRC	0.599	NUFIP2	0.596	CNNM4	0.592	UVRAG	0.592	MSR1	0.589	CYB5B	0.586
ATP1B3	0.605	SMYD2	0.605	NUP85	0.602	DERA	0.599	TIMM44	0.599	NVL	0.596	CNST	0.592	VIM	0.592	MYO1D	0.589	CYTH2	0.586
ATRX	0.605	SRPK2	0.605	PFKP	0.602	DHRS7	0.599	TIMP3	0.599	OSBPL1A	0.596	CYB5R3	0.592	VPS53	0.592	NARF	0.589	CYTIP	0.586
ATXN2	0.605	SSR1	0.605	PGAM1	0.602	EMP1	0.599	TMEM131	0.599	OSGIN2	0.596	DAAM1	0.592	WARS2	0.592	NCOA7	0.589	DCAF8	0.586
AVL9	0.605	STX16-NPEPL1	0.605	PKD2	0.602	FKBP9	0.599	TOMM22	0.599	PAFAH2	0.596	DCAKD	0.592	WDFY3	0.592	NCOR1	0.589	DDX60	0.586
C1orf52	0.605	SUOX	0.605	POLR2K	0.602	FMNL3	0.599	TRAF5	0.599	PCGF5	0.596	DCBLD2	0.592	XRN1	0.592	NIPAL2	0.589	DGUOK	0.586
C7orf60	0.605	TANC1	0.605	PRKCD	0.602	FRA10AC1	0.599	TRAPPC10	0.599	PDCD10	0.596	DMXL2	0.592	YWHAE	0.592	NPL	0.589	DRG1	0.586
CAPN1	0.605	TANC2	0.605	PRPF40A	0.602	FUBP1	0.599	UBQLN2	0.599	PLEKHM2	0.596	DNM2	0.592	ZNF277	0.592	NUP93	0.589	ERBB2IP	0.586
CCDC104	0.605	TBC1D10B	0.605	PSMD14	0.602	GBF1	0.599	UBR2	0.599	PPP1R13B	0.596	ELL2	0.592	ZNF644	0.592	PAIP2	0.589	FAM126A	0.586
CCDC82	0.605	TEAD1	0.605	PTPRS	0.602	GPD2	0.599	UTP11L	0.599	PRPF18	0.596	ENTPD1	0.592	ABCD3	0.589	PDIA6	0.589	FAM49B	0.586
CD46	0.605	TPP2	0.605	RAB22A	0.602	GRAMD4	0.599	VEZT	0.599	PRPF6	0.596	EPS8	0.592	ACSL1	0.589	PERP	0.589	FARP1	0.586
CNIH4	0.605	TRMU	0.605	RALGAPA2	0.602	GRK6	0.599	VKORC1L1	0.599	RBM6	0.596	GLG1	0.592	ACTB	0.589	PHF20	0.589	GIT1	0.586
COIL	0.605	TUBA1C	0.605	RASA2	0.602	GSTCD	0.599	WDR26	0.599	RPRD1B	0.596	HIP1	0.592	ADSS	0.589	PIGT	0.589	GLTSCR2	0.586
COMMD10	0.605	TXLNA	0.605	RHOQ	0.602	HDHD3	0.599	WDR70	0.599	RUNDC1	0.596	IFT122	0.592	ALAD	0.589	PLXNA3	0.589	GNPDA1	0.586
CSTF3	0.605	UBE2D1	0.605	RIN2	0.602	HMGCS1	0.599	YES1	0.599	SAFB	0.596	IL4R	0.592	ANAPC5	0.589	POLDIP2	0.589	GSS	0.586
DCP2	0.605	UNC13B	0.605	RPL28	0.602	HNRNPUL1	0.599	ZAK	0.599	SCAMP4	0.596	KDM4C	0.592	APPBP2	0.589	PRMT2	0.589	HIP1R	0.586
DDX54	0.605	VHL	0.605	SAP30L	0.602	IFFO2	0.599	ZBTB11	0.599	SEC61G	0.596	KIAA0020	0.592	APPL1	0.589	PRPF3	0.589	HSD17B11	0.586
DHRS3	0.605	XPNPEP3	0.605	SEL1L3	0.602	IGBP1	0.599	ZC3H6	0.599	SHC1	0.596	KIAA2018	0.592	ARID4B	0.589	RBM25	0.589	IFIH1	0.586
DIS3L2	0.605	ZFYVE16	0.605	SEPN1	0.602	JAZF1	0.599	ZNF195	0.599	SKIL	0.596	KLHL24	0.592	ATN1	0.589	RBMX	0.589	IGF2R	0.586
DNPEP	0.605	ZMYM3	0.605	SERINC5	0.602	KCNS3	0.599	ZNRF2	0.599	SKIV2L2	0.596	LMO7	0.592	ATP2A2	0.589	RETSAT	0.589	IKBKAP	0.586
DYRK2	0.605	ZMYND8	0.605	SH3TC1	0.602	KIAA1217	0.599	ABCA1	0.596	SLC25A1	0.596	LRRC41	0.592	ATR	0.589	RMND5A	0.589	INPP5B	0.586
EHD4	0.605	ZNF138	0.605	SIPA1	0.602	KLF13	0.599	ANAPC2	0.596	SMEK1	0.596	LSM5	0.592	CACYBP	0.589	RNF139	0.589	KIAA0391	0.586
EIF1AX	0.605	ABHD2	0.602	SKI	0.602	LANCL1	0.599	ARAP2	0.596	SNX19	0.596	LTN1	0.592	CBX5	0.589	SCAMP1	0.589	KIAA0930	0.586

FAM193B	0.605	ADO	0.602	SLC11A2	0.602	LENG8	0.599	ARHGAP18	0.596	SOCS5	0.596	MAPK13	0.592	CCDC14	0.589	SDC4	0.589	KIAA1147	0.586
FBXL5	0.605	AGAP1	0.602	SMCR8	0.602	MAST4	0.599	ARHGDIB	0.596	SORL1	0.596	MAT2B	0.592	CDC14B	0.589	SEC24B	0.589	KLF3	0.586
FYCO1	0.605	ARHGEF18	0.602	SPG11	0.602	MEF2A	0.599	C9orf91	0.596	SUPT5H	0.596	MCPH1	0.592	CFLAR	0.589	SERBP1	0.589	LARP1B	0.586
GALNT10	0.605	ARID4A	0.602	SRRT	0.602	MEN1	0.599	CCDC93	0.596	TACC2	0.596	MORC2	0.592	CLK1	0.589	SETD1B	0.589	LBR	0.586
GALNT2	0.605	ASCC3	0.602	ST5	0.602	MNAT1	0.599	CD2AP	0.596	TIA1	0.596	MPV17	0.592	CNOT6L	0.589	SETD7	0.589	LDOC1L	0.586
GNA11	0.605	ATG14	0.602	STK35	0.602	MORC3	0.599	CDC42BPB	0.596	TLR2	0.596	MSL2	0.592	COPS5	0.589	SLC30A7	0.589	LMBRD1	0.586
GNPTG	0.605	AZIN1	0.602	TCF3	0.602	NCKAP1L	0.599	CEP57L1	0.596	TNFSF10	0.596	NDUFB5	0.592	CRY2	0.589	SLC30A9	0.589	LRP10	0.586
GOLM1	0.605	BTBD3	0.602	TECR	0.602	NOL8	0.599	CKAP2	0.596	TRAPPC3	0.596	NFX1	0.592	CTSH	0.589	SLC38A6	0.589	LYZ	0.586
ID1	0.605	C8orf4	0.602	TIPARP	0.602	PARP8	0.599	COL4A3BP	0.596	TRAPPC9	0.596	NOL6	0.592	DCTN5	0.589	SMG6	0.589	MAML2	0.586
ISCU	0.605	CARS2	0.602	TMEM120B	0.602	PDCL	0.599	COPS7B	0.596	TRPC4AP	0.596	OTUD7B	0.592	DDX47	0.589	STUB1	0.589	MAPK6	0.586
KLC1	0.605	CHD7	0.602	TP53BP1	0.602	PDS5B	0.599	EML2	0.596	VPS13C	0.596	OXR1	0.592	DNAJB14	0.589	SUCLG2	0.589	MATR3	0.586
LIMS1	0.605	CSGALNACT2	0.602	TYK2	0.602	PHLDA1	0.599	EXOC7	0.596	WDR82	0.596	PHLDB2	0.592	DUSP22	0.589	TBC1D16	0.589	MCM5	0.586
M6PR	0.605	DCAF6	0.602	UGCG	0.602	PPFIA1	0.599	FAM122B	0.596	ZBTB38	0.596	PHRF1	0.592	EAPP	0.589	TBC1D19	0.589	MDH2	0.586
MFN1	0.605	DECR1	0.602	UQCR10	0.602	PPIB	0.599	FAM129A	0.596	ZW10	0.596	PI4KA	0.592	EFTUD2	0.589	TTC1	0.589	MGLL	0.586
MIA3	0.605	DHX29	0.602	USO1	0.602	PPIE	0.599	FNDC3A	0.596	ABCD4	0.592	PLAU	0.592	EIF3B	0.589	TTL	0.589	MRPL34	0.586
MYO19	0.605	DOCK10	0.602	WDR7	0.602	PPIG	0.599	GNS	0.596	ACTN4	0.592	RAD23A	0.592	EPC2	0.589	UBAP2	0.589	MRPL9	0.586
NCL	0.605	ELL	0.602	WEE1	0.602	PREX1	0.599	GPBP1L1	0.596	AGGF1	0.592	RARRES3	0.592	FAM120B	0.589	USP45	0.589	MUM1	0.586
NOP56	0.605	EP300	0.602	WWC3	0.602	PSMD3	0.599	GRPEL1	0.596	AGPS	0.592	RARS	0.592	FAM46C	0.589	WARS	0.589	NAGA	0.586
NUP210	0.605	EPM2AIP1	0.602	ZC3H11A	0.602	PWWP2A	0.599	HARS	0.596	AKT2	0.592	RNPEPL1	0.592	FOXK1	0.589	ZFYVE26	0.589	NKAP	0.586
PCF11	0.605	ERAP1	0.602	ZCCHC11	0.602	RAB12	0.599	HIBADH	0.596	ALDOA	0.592	SARS	0.592	FRMD4B	0.589	ZMAT3	0.589	NOTCH3	0.586
PCGF3	0.605	EZR	0.602	ZNF326	0.602	RAB40C	0.599	HINT3	0.596	APOC1	0.592	SF3A1	0.592	FXR1	0.589	ZNF207	0.589	PCBP2	0.586
PDS5A	0.605	FZD4	0.602	ADD1	0.599	RAD17	0.599	HNRNPM	0.596	ARFGAP3	0.592	SKP1	0.592	GSTP1	0.589	ZNF318	0.589	PDCD6IP	0.586
PIAS1	0.605	HAUS6	0.602	ANKRD44	0.599	RANBP2	0.599	IFI44	0.596	ARID1B	0.592	SLC38A10	0.592	HECTD1	0.589	ZNF37A	0.589	PHAX	0.586
PHKB	0.586	EIF2AK3	0.583	ZNF25	0.583	PATL1	0.580	DOCK7	0.577	RNF13	0.577	KHSRP	0.574	TOR3A	0.574	IDH3B	0.571	APOA1BP	0.567
PIGS	0.586	EIF3D	0.583	ZNF407	0.583	PCMTD2	0.580	DSTN	0.577	RPS19BP1	0.577	KIAA0753	0.574	TPD52	0.574	ITM2C	0.571	ASB3	0.567
PNRC1	0.586	ERLEC1	0.583	ZNF7	0.583	PCNP	0.580	DUSP11	0.577	S100A9	0.577	KIAA1522	0.574	TPM2	0.574	JAG1	0.571	ATM	0.567
PRKCA	0.586	EXOC6B	0.583	ACTN1	0.580	PDXDC2P	0.580	EIF4B	0.577	SAMD12	0.577	KITLG	0.574	TPST1	0.574	KDM5A	0.571	C1orf123	0.567
PSMA3	0.586	FHOD1	0.583	ADAM17	0.580	PHACTR4	0.580	EVI5	0.577	SAMSN1	0.577	LAMA5	0.574	UBA2	0.574	KDM5B	0.571	C20orf194	0.567
R3HDM2	0.586	G3BP1	0.583	AKT1	0.580	PLEKHB2	0.580	EYA3	0.577	SDPR	0.577	LARS	0.574	UGGT2	0.574	KIF5B	0.571	C2orf68	0.567
RAVER1	0.586	GOLGA5	0.583	ALPK1	0.580	POLR2B	0.580	FCHO2	0.577	SHPRH	0.577	LOC283922	0.574	ZBTB7B	0.574	LRRC8D	0.571	CASP10	0.567
RBPMS	0.586	H2AFV	0.583	ATG3	0.580	POLR3E	0.580	FMN1	0.577	SLC12A4	0.577	LRCH4	0.574	ZCCHC6	0.574	MAPK1	0.571	CCND1	0.567
RHOC	0.586	HMBOX1	0.583	ATP5G3	0.580	PPP2R5A	0.580	FRYL	0.577	SP3	0.577	LTA4H	0.574	ZNF700	0.574	MDH1	0.571	CDC123	0.567
RNF10	0.586	HNMT	0.583	ATP9B	0.580	PRCC	0.580	FUNDC2	0.577	TARDBP	0.577	MAP3K5	0.574	ACOT9	0.571	MGAT4B	0.571	CDC5L	0.567
RPS23	0.586	IGHMBP2	0.583	C11orf24	0.580	PRDX4	0.580	GAK	0.577	TSN	0.577	MAPKAPK5	0.574	ADCY7	0.571	MIER1	0.571	CEP164	0.567
RRAGC	0.586	ITGA5	0.583	CCDC80	0.580	PRR14	0.580	GANAB	0.577	UBE3A	0.577	MAST2	0.574	ANAPC16	0.571	MIOS	0.571	CLIC4	0.567
SDCBP	0.586	JUP	0.583	CCNB1IP1	0.580	PSKH1	0.580	GAPVD1	0.577	UGP2	0.577	MBD3	0.574	ANKRD11	0.571	MRPL13	0.571	COL1A1	0.567
SEMA4D	0.586	KIAA0430	0.583	CDC34	0.580	PSMB1	0.580	GARS	0.577	USP4	0.577	MGST3	0.574	ANKRD26	0.571	MZT2B	0.571	COQ4	0.567
SH3GLB1	0.586	LMAN1	0.583	CELF2	0.580	PSMD12	0.580	GLUL	0.577	VPS29	0.577	MRPL23	0.574	ANKRD36B	0.571	NPC2	0.571	COX5B	0.567
SLC12A6	0.586	MAN2B2	0.583	COG2	0.580	PSMD4	0.580	GOT2	0.577	XAB2	0.577	MRPL37	0.574	ARFGAP2	0.571	NUCKS1	0.571	CPNE3	0.567

SLC25A36	0.586	MAP7	0.583	CTBP1	0.580	PYCR2	0.580	HDAC1	0.577	ZNF841	0.577	NCBP1	0.574	ATP7A	0.571	NUP107	0.571	DAB2	0.567
SNX1	0.586	MEIS1	0.583	CUL7	0.580	RAB23	0.580	HDAC2	0.577	AGRN	0.574	NDRG1	0.574	ATXN7L3	0.571	PCMTD1	0.571	DCUN1D5	0.567
SPG20	0.586	MGAT4A	0.583	CWC22	0.580	RASSF1	0.580	HEATR5B	0.577	ANKLE2	0.574	NDUFB4	0.574	BAZ2B	0.571	PDLIM5	0.571	DNAJC13	0.567
SPRY1	0.586	MORF4L1	0.583	CWC25	0.580	RBCK1	0.580	IFT57	0.577	ANXA2	0.574	NDUFS5	0.574	C16orf80	0.571	PHF23	0.571	ECHDC2	0.567
SYAP1	0.586	MTHFD1L	0.583	DCTD	0.580	REST	0.580	IK	0.577	AP1G2	0.574	NFYB	0.574	C17orf62	0.571	PIK3R1	0.571	EIF3F	0.567
TGS1	0.586	NARG2	0.583	DHX57	0.580	RHOB	0.580	INO80	0.577	ARHGEF10L	0.574	NOL10	0.574	C21orf33	0.571	PITPNB	0.571	ERCC3	0.567
TMEM63B	0.586	NDUFA9	0.583	DPP8	0.580	RHOB	0.580	IPO11	0.577	ARID1A	0.574	NT5C2	0.574	CALD1	0.571	PON2	0.571	EVC	0.567
UBE2I	0.586	OPA1	0.583	DUSP6	0.580	RNF111	0.580	IQCB1	0.577	ATF7IP2	0.574	NUP54	0.574	CARS	0.571	PPAP2B	0.571	EXOSC10	0.567
UBE3C	0.586	PARP2	0.583	ECHS1	0.580	RREB1	0.580	IRAK3	0.577	BCAT2	0.574	PHF2	0.574	CEP57	0.571	RHBDF2	0.571	FBXL20	0.567
UBE4B	0.586	PIK3C2A	0.583	FBXO18	0.580	SAP18	0.580	KCTD10	0.577	BTBD10	0.574	PITPNM1	0.574	CHM	0.571	RPS14	0.571	FGD6	0.567
UBXN4	0.586	PPM1B	0.583	FBXW5	0.580	SECISBP2	0.580	KIAA1468	0.577	BTBD6	0.574	PLAGL2	0.574	CLEC2B	0.571	SCFD2	0.571	FGFR1OP	0.567
UHRF1BP1	0.586	PPP2R2A	0.583	FLNA	0.580	SNX33	0.580	LIG3	0.577	CCDC12	0.574	PLEKHA1	0.574	COL6A3	0.571	SEC63	0.571	FMNL1	0.567
VPS13B	0.586	PSMA4	0.583	FNBP4	0.580	SPATA20	0.580	LMCD1	0.577	CCDC88C	0.574	PLS3	0.574	COPS2	0.571	SEPW1	0.571	GOLGA1	0.567
VPS35	0.586	PTER	0.583	FNIP2	0.580	SPATA5	0.580	LRP5	0.577	CDK16	0.574	PPP1R15A	0.574	COQ10B	0.571	SLC25A37	0.571	GPR56	0.567
YTHDF2	0.586	REPIN1	0.583	FOXP1	0.580	SREK1	0.580	LSM4	0.577	CHST15	0.574	PRKRIR	0.574	CSNK1G3	0.571	SORD	0.571	HIST1H4C	0.567
ZNF24	0.586	RFX7	0.583	GAPDH	0.580	SRSF8	0.580	MAP3K8	0.577	CHSY1	0.574	PRMT3	0.574	CTGF	0.571	SPPL2A	0.571	IFITM3	0.567
ABCC10	0.583	RMRP	0.583	GRWD1	0.580	STX7	0.580	MARS	0.577	CIITA	0.574	PRPF19	0.574	CTNNBIP1	0.571	SRFBP1	0.571	IMP3	0.567
ABCG1	0.583	SEC24A	0.583	GTF3C6	0.580	TAOK1	0.580	MAT2A	0.577	CLIP4	0.574	PTK2B	0.574	CYTH3	0.571	SUGT1	0.571	ITGA1	0.567
AFF1	0.583	SECISBP2L	0.583	GTPBP1	0.580	TBCCD1	0.580	MERTK	0.577	COPS4	0.574	RASA1	0.574	DCK	0.571	TERF2	0.571	KCMF1	0.567
ALAS1	0.583	SETD2	0.583	HECTD3	0.580	TET2	0.580	MRPS27	0.577	CTDSPL	0.574	RBM19	0.574	DDX23	0.571	TGOLN2	0.571	KDM5C	0.567
AMOTL2	0.583	SLC38A1	0.583	HOOK3	0.580	TRIM22	0.580	NBPF15	0.577	CTSC	0.574	RSBN1L	0.574	DNAJC3	0.571	TMEM18	0.571	KPNA2	0.567
ANKRD36	0.583	SMAD2	0.583	IDH3A	0.580	TRRAP	0.580	NINJ1	0.577	CYR61	0.574	SDC3	0.574	DOCK1	0.571	TMEM59	0.571	LSM14B	0.567
ATAD2	0.583	SPAG9	0.583	IGFBP3	0.580	TSKU	0.580	NRP1	0.577	DICER1	0.574	SERTAD2	0.574	DSP	0.571	TNFRSF14	0.571	LUC7L2	0.567
AZI2	0.583	SPARCL1	0.583	INVS	0.580	TTC12	0.580	NUCB1	0.577	DPH1	0.574	SLFN11	0.574	DYNC1H1	0.571	TTC13	0.571	MAP3K1	0.567
B4GALT3	0.583	SSFA2	0.583	ITGA2	0.580	UBTF	0.580	NUP98	0.577	EFHD2	0.574	SMAD4	0.574	DYRK1A	0.571	TUBA4A	0.571	MED10	0.567
BCLAF1	0.583	ST6GAL1	0.583	IWS1	0.580	USPL1	0.580	OBFC1	0.577	EHD2	0.574	SMPD4	0.574	EIF2AK1	0.571	TULP4	0.571	MED21	0.567
C15orf39	0.583	STRN4	0.583	KIAA0556	0.580	VOPP1	0.580	OTUD3	0.577	EIF4G1	0.574	SNW1	0.574	ELP4	0.571	TXNDC15	0.571	MRFAP1	0.567
C1QB	0.583	STT3A	0.583	KIF2A	0.580	VRK2	0.580	PDPR	0.577	EPG5	0.574	SOD1	0.574	ETAA1	0.571	UBFD1	0.571	MYCBP2	0.567
CAD	0.583	STXBP4	0.583	KNTC1	0.580	WNK1	0.580	PI4K2B	0.577	ETS2	0.574	STAM	0.574	FAM160B2	0.571	UBR3	0.571	MYLK	0.567
CCDC53	0.583	SYPL1	0.583	LARP1	0.580	ZFP62	0.580	PICALM	0.577	FAM120A	0.574	STMN1	0.574	FAM3C	0.571	UBXN7	0.571	N4BP2	0.567
CCT3	0.583	TARBP1	0.583	LPP	0.580	ZNF496	0.580	PIP5K1A	0.577	FAM35A	0.574	STX8	0.574	FBXW7	0.571	ULK1	0.571	NDUFS2	0.567
CDK2AP1	0.583	TMCO1	0.583	MANBA	0.580	AAAS	0.577	PML	0.577	FBXO31	0.574	SUV420H1	0.574	FILIP1L	0.571	WDR1	0.571	NPLOC4	0.567
CHURC1	0.583	TMCO3	0.583	MAPKAP1	0.580	APPL2	0.577	PMPCA	0.577	GCLM	0.574	TBC1D13	0.574	FOXJ3	0.571	ZBTB40	0.571	NRBP1	0.567
CLTA	0.583	TMEM135	0.583	MBD5	0.580	ATF4	0.577	PMS1	0.577	GGPS1	0.574	TBC1D22A	0.574	GAA	0.571	ZNF276	0.571	PAK4	0.567
CORO1B	0.583	TMEM209	0.583	ME2	0.580	BIRC6	0.577	PSD3	0.577	GOLGA4	0.574	TCERG1	0.574	GLO1	0.571	ZNF512	0.571	PHC3	0.567
CPSF7	0.583	TMX3	0.583	MGA	0.580	C7orf50	0.577	PSMD1	0.577	GRINA	0.574	TCF4	0.574	GNPAT	0.571	ZNF518A	0.571	PIGO	0.567
CTNNAL1	0.583	TTLL5	0.583	NACC1	0.580	CETN2	0.577	RABEP1	0.577	GRSF1	0.574	THOC5	0.574	GORAB	0.571	ZNF577	0.571	POGZ	0.567
DAZAP1	0.583	TXN2	0.583	NAE1	0.580	CFL1	0.577	RAF1	0.577	HAUS4	0.574	TM2D1	0.574	GTF3C2	0.571	ACLY	0.567	PPP1CB	0.567
DDX24	0.583	UQCRB	0.583	NAPA	0.580	COPS8	0.577	RAP2B	0.577	HERC3	0.574	TMBIM4	0.574	GUK1	0.571	ACSF3	0.567	RABAC1	0.567

DENND1A	0.583	UTRN	0.583	NIF3L1	0.580	CRBN	0.577	RAPGEF6	0.577	INO80D	0.574	TMEM164	0.574	HNRNPR	0.571	ACSL3	0.567	RGS1	0.567
DPYD	0.583	WDR60	0.583	NPNT	0.580	DHDDS	0.577	RBPJ	0.577	IPO8	0.574	TMEM184C	0.574	HYOU1	0.571	ALG13	0.567	RPS27L	0.567
ECI2	0.583	YPEL5	0.583	PARP3	0.580	DMXL1	0.577	REV3L	0.577	JOSD1	0.574	TOR1AIP2	0.574	IARS2	0.571	ANKRD10	0.567	RSRC1	0.567
RTF1	0.567	DCAF13	0.564	COMT	0.564	DNAJC11	0.561	RNPS1	0.561	CSRP1	0.558	RPL27	0.558	CD63	0.555	RSU1	0.555	DDB1	0.552
SDF4	0.567	DDX18	0.564	CYBA	0.564	EEF2	0.561	RPS15A	0.561	CTSB	0.558	RRAS2	0.558	CD9	0.555	SIK3	0.555	DERL2	0.552
SELK	0.567	DKC1	0.564	DENR	0.564	ELAC2	0.561	RPS19	0.561	DARS	0.558	RUFY2	0.558	CDC40	0.555	SLC27A4	0.555	DLEU2	0.552
SF3B2	0.567	DLD	0.564	EHBP1	0.564	FBRSL1	0.561	RPTOR	0.561	DEAF1	0.558	SAR1A	0.558	COTL1	0.555	SMS	0.555	EEF2K	0.552
SGTA	0.567	DNAJC5	0.564	ENO2	0.564	FIBP	0.561	RTKN	0.561	DGCR2	0.558	SCP2	0.558	COX5A	0.555	SNAP29	0.555	EGLN1	0.552
SHQ1	0.567	DPYSL2	0.564	ERGIC3	0.564	GAB1	0.561	SCARNA5	0.561	DIDO1	0.558	SDHAP2	0.558	DNAJA1	0.555	SNAPC3	0.555	EIF4ENIF1	0.552
SLC16A3	0.567	DZIP3	0.564	HIST1H4B	0.564	GDI1	0.561	SENP7	0.561	DNAJB2	0.558	SERPING1	0.558	EGR1	0.555	SNORA37	0.555	ERH	0.552
SLC30A5	0.567	E4F1	0.564	ING4	0.564	GNB2	0.561	SF3B1	0.561	DPYSL3	0.558	SLC35C1	0.558	EIF4E3	0.555	SNRPD1	0.555	ESYT1	0.552
SLTM	0.567	ERCC6	0.564	LRRC8A	0.564	GOLIM4	0.561	SH3GL1	0.561	DUSP3	0.558	SLC44A2	0.558	ELMO1	0.555	SPARC	0.555	FAT1	0.552
SOCS3	0.567	FLOT2	0.564	MXD1	0.564	HDDC2	0.561	SH3YL1	0.561	EIF3E	0.558	SMC4	0.558	FAM118A	0.555	SPATS2	0.555	FCGRT	0.552
SPTAN1	0.567	FRG1	0.564	NF2	0.564	HGS	0.561	SLC22A23	0.561	EIF4E2	0.558	SPCS1	0.558	FBXL4	0.555	SSH1	0.555	FDPS	0.552
STARD3NL	0.567	GART	0.564	NHLRC2	0.564	HMGN4	0.561	SMARCA4	0.561	EIF5A	0.558	SPCS2	0.558	FBXO11	0.555	TCTN3	0.555	FOXN2	0.552
SYNE2	0.567	GCC1	0.564	NME4	0.564	HN1	0.561	SOS1	0.561	ENTPD6	0.558	SPCS3	0.558	FBXO8	0.555	TDP2	0.555	GADD45B	0.552
TALDO1	0.567	JAK3	0.564	PER2	0.564	HPCAL1	0.561	SP1	0.561	ERP44	0.558	SPIN1	0.558	FECH	0.555	TGIF1	0.555	GEMIN8	0.552
TDRD3	0.567	LHFP	0.564	PTK7	0.564	HSF1	0.561	STRN	0.561	FARSA	0.558	SRGAP1	0.558	FKBP5	0.555	TIPRL	0.555	GMPPA	0.552
TERF2IP	0.567	LSM14A	0.564	RIOK1	0.564	IDE	0.561	SUN2	0.561	FBXO9	0.558	SRP72	0.558	FRS2	0.555	TM9SF3	0.555	GOLGA3	0.552
THRA	0.567	MAGED1	0.564	RNF187	0.564	IDH2	0.561	TBCB	0.561	FLII	0.558	SRSF9	0.558	GPNMB	0.555	TNPO1	0.555	HMGXB3	0.552
TMEM123	0.567	MKL2	0.564	SF1	0.564	IGJ	0.561	TBL1XR1	0.561	FNTA	0.558	SYF2	0.558	GTPBP10	0.555	TP53	0.555	HPRT1	0.552
TMOD3	0.567	MLLT10	0.564	SHISA5	0.564	IL1R1	0.561	TBL2	0.561	GPS1	0.558	TBC1D15	0.558	HMGB2	0.555	TRANK1	0.555	ILK	0.552
TSC1	0.567	MTUS1	0.564	SRC	0.564	IMPAD1	0.561	TMBIM1	0.561	GSK3B	0.558	TBC1D20	0.558	HTRA1	0.555	TRIM44	0.555	INSR	0.552
TTC21B	0.567	N4BP2L2	0.564	STIM1	0.564	KDM1A	0.561	TMCC1	0.561	GTF2F1	0.558	TBCEL	0.558	IARS	0.555	TSPYL4	0.555	INTS6	0.552
TUG1	0.567	NBAS	0.564	THAP4	0.564	KDM2B	0.561	TMEM41B	0.561	HBS1L	0.558	THADA	0.558	IFNGR1	0.555	TTC37	0.555	IRGQ	0.552
UACA	0.567	NBEAL1	0.564	TMEM127	0.564	KIF1C	0.561	TMEM62	0.561	HDAC6	0.558	THUMPD1	0.558	IFNGR2	0.555	TUBGCP5	0.555	ITFG3	0.552
UBE2D3	0.567	NDUFA1	0.564	TMEM167B	0.564	LMO4	0.561	TNC	0.561	HIATL1	0.558	TIMP1	0.558	IL17RA	0.555	VAT1	0.555	KIF16B	0.552
UFSP2	0.567	NDUFA4	0.564	TMEM214	0.564	LRPPRC	0.561	TPCN1	0.561	HMGXB4	0.558	TJAP1	0.558	ITPKB	0.555	VBP1	0.555	LDHB	0.552
VPS18	0.567	NUP205	0.564	TRIM25	0.564	LRRCC1	0.561	TPM1	0.561	HMOX2	0.558	TM4SF1	0.558	IVNS1ABP	0.555	WDR73	0.555	LOC550643	0.552
VTI1A	0.567	NXN	0.564	TSPO	0.564	LYRM2	0.561	TRAF2	0.561	HNRNPD	0.558	TNFAIP3	0.558	KIAA0368	0.555	YWHAG	0.555	LRRFIP1	0.552
WBSCR22	0.567	ODF2L	0.564	UBE3B	0.564	MAPK14	0.561	TRAK2	0.561	IQGAP1	0.558	TRPS1	0.558	KIAA1033	0.555	ZNF664	0.555	LTBP4	0.552
WWOX	0.567	PCCA	0.564	UNC45A	0.564	MARVELD1	0.561	TRIM65	0.561	KHDRBS1	0.558	TSPAN3	0.558	KLF9	0.555	ZNF680	0.555	LZTR1	0.552
XPO4	0.567	PHF3	0.564	ZNF641	0.564	MBD2	0.561	UFC1	0.561	KIAA0247	0.558	TTLL4	0.558	KLHL36	0.555	ZNHIT1	0.555	MAGI3	0.552
XPOT	0.567	PPP1R13L	0.564	AGPAT6	0.561	MED14	0.561	VPS13D	0.561	KIAA1430	0.558	TXNL1	0.558	LATS1	0.555	ABR	0.552	MAN2A1	0.552
XRCC6	0.567	RAB11FIP2	0.564	AIM1	0.561	MLXIP	0.561	XAF1	0.561	KIAA1919	0.558	UHMK1	0.558	LEO1	0.555	ACIN1	0.552	MAP2K5	0.552
YIPF5	0.567	RAD23B	0.564	APBB2	0.561	MRPL32	0.561	YWHAZ	0.561	KRT18	0.558	UQCRH	0.558	LIMA1	0.555	ADRBK1	0.552	MCM7	0.552
ZHX3	0.567	RBBP6	0.564	APEH	0.561	MTCH1	0.561	ZCCHC14	0.561	MAML1	0.558	VPS13A	0.558	LUZP1	0.555	ANP32A	0.552	MEX3C	0.552
ZKSCAN1	0.567	RRAS	0.564	ARL1	0.561	MXI1	0.561	ZDHHC5	0.561	MBNL2	0.558	VPS39	0.558	MDN1	0.555	APOL2	0.552	MGEA5	0.552
ZNF609	0.567	SAMHD1	0.564	ARMC10	0.561	NCK2	0.561	ZNF330	0.561	MCM3AP	0.558	WDR41	0.558	MED15	0.555	ARHGEF1	0.552	MRPL16	0.552

ABL1	0.564	SCAF1	0.564	ATF1	0.561	NUMB	0.561	ZNF335	0.561	MRPS10	0.558	WDR59	0.558	MRFAP1L1	0.555	ARL4C	0.552	MSL1	0.552
ADAM15	0.564	SH3BP4	0.564	BRD8	0.561	NUTF2	0.561	ZNF460	0.561	NECAP1	0.558	YBX1	0.558	MRPL27	0.555	ATF2	0.552	MTMR10	0.552
AHCTF1	0.564	SMG5	0.564	BTG2	0.561	OTUD4	0.561	ANKFY1	0.558	NOP58	0.558	YPEL3	0.558	NAA25	0.555	ATP6V0E1	0.552	NAA10	0.552
AKAP1	0.564	SNX29	0.564	C17orf85	0.561	PAN2	0.561	ARHGAP23	0.558	PER1	0.558	ZDHHC17	0.558	NDUFB2	0.555	ATP6V1A	0.552	NAP1L4	0.552
APC	0.564	TBCA	0.564	C1QTNF3-AMACR	0.561	PARP9	0.561	ASAP2	0.558	PHF8	0.558	ZDHHC7	0.558	NOL11	0.555	BABAM1	0.552	NCAPD3	0.552
ARHGEF12	0.564	TCEA1	0.564	C1R	0.561	PAWR	0.561	ATP11C	0.558	PLD3	0.558	ZNF302	0.558	NR2C2	0.555	BARD1	0.552	NDUFA11	0.552
ARL8A	0.564	TEX2	0.564	CAMK2D	0.561	PI4KB	0.561	ATP6V1F	0.558	PLOD1	0.558	ZNF445	0.558	NUCB2	0.555	BAX	0.552	NET1	0.552
ATAD2B	0.564	TFCP2	0.564	CARM1	0.561	PITPNA	0.561	ATXN7L3B	0.558	PPP1R2	0.558	ZNF791	0.558	ODF2	0.555	BCAR1	0.552	NFIB	0.552
AUH	0.564	TIMP2	0.564	CCNG2	0.561	PKN2	0.561	BCOR	0.558	PPP3CC	0.558	ZXDC	0.558	OSTC	0.555	BCL2L13	0.552	NIN	0.552
BAZ1A	0.564	TRIM24	0.564	CD74	0.561	PLEKHA7	0.561	CAST	0.558	PRH1-PRR4	0.558	ADNP	0.555	PFKFB2	0.555	BTBD1	0.552	NUDT5	0.552
BAZ2A	0.564	UBE2L6	0.564	CDKAL1	0.561	POGK	0.561	CD82	0.558	PRKAB1	0.558	ADPGK	0.555	PHF14	0.555	C11orf58	0.552	PAK2	0.552
BCL3	0.564	UEVLD	0.564	CEBPG	0.561	POLD3	0.561	CENPJ	0.558	PRKAR1A	0.558	ALDH9A1	0.555	PIM1	0.555	CANT1	0.552	PDCD7	0.552
CASC3	0.564	WDR13	0.564	CLN3	0.561	POLE3	0.561	CLDND1	0.558	PSME1	0.558	ANKRD13D	0.555	PLSCR1	0.555	CAP1	0.552	PELP1	0.552
CASP8	0.564	ZFC3H1	0.564	CMTM6	0.561	POLR2C	0.561	CLK4	0.558	PSME2	0.558	BLVRA	0.555	PPP1R8	0.555	CASK	0.552	PGLS	0.552
CBX1	0.564	ZNF76	0.564	CPPED1	0.561	PPP6R3	0.561	CMPK1	0.558	PTP4A1	0.558	C10orf11	0.555	PRKCSH	0.555	CCDC47	0.552	PHB2	0.552
CBX7	0.564	ZNF800	0.564	CRIM1	0.561	PTEN	0.561	COL4A2	0.558	PTP4A2	0.558	C14orf166	0.555	PSMF1	0.555	CCDC69	0.552	PIH1D1	0.552
CCDC43	0.564	ZYG11B	0.564	CSNK1G2	0.561	PUM2	0.561	COPB1	0.558	PTPRC	0.558	CC2D1B	0.555	RAD54L2	0.555	CDC42	0.552	PJA2	0.552
CCDC90B	0.564	ZZZ3	0.564	CTSZ	0.561	PXN	0.561	COX17	0.558	RAB3GAP2	0.558	CCNL1	0.555	RBBP8	0.555	CDV3	0.552	PLCB3	0.552
CDK12	0.564	ADAT1	0.564	CUL4A	0.561	RC3H2	0.561	CPSF6	0.558	RBM39	0.558	CCNT1	0.555	RBBP9	0.555	CHMP1A	0.552	PMPCB	0.552
COPS3	0.564	ANKZF1	0.564	DDX21	0.561	RDH10	0.561	CREBBP	0.558	RHBDD2	0.558	CCNT2	0.555	RCC1	0.555	CLTC	0.552	POT1	0.552
CTC1	0.564	AP2A1	0.564	DENND5A	0.561	RFK	0.561	CRK	0.558	RHOG	0.558	CCT5	0.555	RIC8A	0.555	CREG1	0.552	PPP6R1	0.552
CTNNBL1	0.564	CCNI	0.564	DIAPH2	0.561	RNF41	0.561	CSE1L	0.558	RNF44	0.558	CD151	0.555	RPL6	0.555	CSNK2A1	0.552	PREB	0.552
PRKRA	0.552	CSK	0.549	SFSWAP	0.549	CPNE2	0.545	PPA2	0.545	CISD2	0.542	RQCD1	0.542	ERP29	0.539	SLC4A2	0.539	CORO1C	0.536
PTAR1	0.552	CST3	0.549	SH3GLB2	0.549	CSNK1G1	0.545	PRICKLE2	0.545	COPB2	0.542	SART3	0.542	F3	0.539	SNRNP200	0.539	CREBL2	0.536
PTPRG	0.552	EBAG9	0.549	SH3PXD2A	0.549	CTDP1	0.545	PRKACA	0.545	CPSF3	0.542	SCPEP1	0.542	FAM162A	0.539	SNX17	0.539	CRELD2	0.536
RAB3GAP1	0.552	EIF2D	0.549	SLC25A24	0.549	CUEDC1	0.545	PRMT1	0.545	CPSF3L	0.542	SERPINB1	0.542	FARSB	0.539	SPATA6	0.539	CSNK1E	0.536
RAN	0.552	FAM127A	0.549	SLFN5	0.549	CWC15	0.545	PSENEN	0.545	CRKL	0.542	SLC12A9	0.542	FRMD8	0.539	SRGN	0.539	CYHR1	0.536
RBM28	0.552	FAM129B	0.549	SMARCB1	0.549	DAB2IP	0.545	PSMC1	0.545	CSNK1A1	0.542	SLC25A28	0.542	GLCE	0.539	SS18L1	0.539	DCTN2	0.536
RPA1	0.552	FAM178A	0.549	SNED1	0.549	DBN1	0.545	PSME4	0.545	DDX51	0.542	SLC35A5	0.542	GMCL1	0.539	TAB1	0.539	DEF8	0.536
SAT2	0.552	FKBP3	0.549	STK17B	0.549	DCUN1D1	0.545	PXDN	0.545	DNAJB11	0.542	SLC50A1	0.542	GTF2H1	0.539	TADA2B	0.539	DEK	0.536
SBF1	0.552	FOS	0.549	STX4	0.549	DDRGK1	0.545	RAB35	0.545	DUSP1	0.542	SLU7	0.542	H2AFZ	0.539	TATDN2	0.539	DGKA	0.536
SIKE1	0.552	GNAI2	0.549	STXBP1	0.549	DNAJB12	0.545	RAI1	0.545	EMP2	0.542	SMARCAD1	0.542	HERC2	0.539	TBC1D5	0.539	DHX15	0.536
SLC12A7	0.552	HDAC3	0.549	SUMO1	0.549	DNAJC8	0.545	RB1	0.545	EPRS	0.542	SMARCD1	0.542	IL1RAP	0.539	TBCC	0.539	DIABLO	0.536
SLC25A3	0.552	HMGB3	0.549	SUPT16H	0.549	DOCK6	0.545	RBBP7	0.545	ERLIN2	0.542	SNAP23	0.542	INTS10	0.539	TFIP11	0.539	DNAJC16	0.536
SLCO3A1	0.552	HNRNPA1	0.549	TARS	0.549	DROSHA	0.545	RBFOX2	0.545	FAM13B	0.542	SOD2	0.542	IRF2BP2	0.539	TPM4	0.539	DRG2	0.536
SMARCC1	0.552	HNRNPC	0.549	TCEB3	0.549	DYNC1I2	0.545	RCAN3	0.545	FAM60A	0.542	SPTLC1	0.542	KDM6A	0.539	TPP1	0.539	EDC3	0.536
SMNDC1	0.552	HOOK2	0.549	TCF20	0.549	DYNLRB1	0.545	RPL38	0.545	FAM76A	0.542	STK4	0.542	KLC2	0.539	TRA2A	0.539	EEF1G	0.536
SPAST	0.552	HTT	0.549	TFPI	0.549	EIF1	0.545	RRM1	0.545	FAS	0.542	STXBP2	0.542	LAPTM5	0.539	TRIM21	0.539	EFEMP1	0.536
SPECC1	0.552	IFIT3	0.549	TM9SF2	0.549	ENGASE	0.545	SCAPER	0.545	FKBP10	0.542	STXBP3	0.542	LARP7	0.539	TRIO	0.539	ERGIC2	0.536

SRP9	0.552	IGF1R	0.549	TNS1	0.549	FAM65A	0.545	SCARNA2	0.545	FUS	0.542	SWAP70	0.542	LMBRD2	0.539	TRPM7	0.539	ERO1L	0.536
SSRP1	0.552	KCTD3	0.549	TRIP4	0.549	FAM73B	0.545	SDAD1	0.545	HEXA	0.542	TAF12	0.542	MAFB	0.539	TSTA3	0.539	EXOSC7	0.536
STEAP3	0.552	KIAA0513	0.549	TWSG1	0.549	FARS2	0.545	SEPHS2	0.545	HSD17B12	0.542	TCP1	0.542	MAP3K11	0.539	UBL4A	0.539	FAM134C	0.536
SYNCRIP	0.552	KIAA0907	0.549	UBE2A	0.549	FBXO7	0.545	SERPINE1	0.545	HSPA4	0.542	TMEM50A	0.542	MAP3K6	0.539	USF2	0.539	FAM8A1	0.536
TIMM50	0.552	KIAA1191	0.549	UBE2E1	0.549	FCHSD2	0.545	SIK1	0.545	ILF3	0.542	TNIP2	0.542	MAP3K7	0.539	USP34	0.539	FN3KRP	0.536
TKT	0.552	KIF13A	0.549	UCKL1	0.549	FOPNL	0.545	SLK	0.545	ITPR3	0.542	UFD1L	0.542	MBNL3	0.539	WBP2	0.539	GABARAPL2	0.536
TRAPPC1	0.552	KLF7	0.549	USP15	0.549	G6PD	0.545	SRSF4	0.545	KIAA1109	0.542	USP21	0.542	MDM4	0.539	WHSC1L1	0.539	GIT2	0.536
TTBK2	0.552	LRIG3	0.549	UTP6	0.549	GAS6	0.545	STK11	0.545	KLHDC3	0.542	USP22	0.542	MMP14	0.539	WTAP	0.539	GLYR1	0.536
U2AF1	0.552	MAP3K4	0.549	VCAN	0.549	GATC	0.545	STOML2	0.545	KPNA6	0.542	VPS28	0.542	MYSM1	0.539	YWHAH	0.539	GNB4	0.536
UNK	0.552	MAP4K3	0.549	VEGFA	0.549	GIPC1	0.545	TECPR2	0.545	KPNB1	0.542	WDR74	0.542	NNMT	0.539	ZFHX3	0.539	GOSR1	0.536
USP16	0.552	MAPRE1	0.549	VMA21	0.549	GLUD1	0.545	TSC22D3	0.545	LIPA	0.542	XPNPEP1	0.542	NUP50	0.539	ZFX	0.539	GSTK1	0.536
USP48	0.552	MFN2	0.549	WDFY2	0.549	GMIP	0.545	TTC7A	0.545	LMNA	0.542	YARS	0.542	OPHN1	0.539	ZMIZ2	0.539	HAGH	0.536
ZBED5	0.552	MON2	0.549	YKT6	0.549	HDLBP	0.545	UBE2V2	0.545	MLF2	0.542	ZEB2	0.542	ORC2	0.539	ZNF384	0.539	HIBCH	0.536
ZFAND1	0.552	NDST1	0.549	ZDHHC16	0.549	HIST1H2BK	0.545	VAMP2	0.545	MSL3	0.542	ZNF598	0.542	OSBP	0.539	ZNF512B	0.539	HIST1H1C	0.536
ZNF394	0.552	NFIA	0.549	ZNF142	0.549	HSD17B10	0.545	WLS	0.545	MTA3	0.542	ABI1	0.539	PAICS	0.539	ZNF622	0.539	HMGB1	0.536
ACADVL	0.549	OAZ2	0.549	ZNF532	0.549	IGFBP7	0.545	ZC3H14	0.545	MTMR2	0.542	ACTL6A	0.539	PCNXL2	0.539	ZNF740	0.539	HNRNPL	0.536
ACTG1	0.549	OGFRL1	0.549	ZNF544	0.549	ING5	0.545	ZMYM4	0.545	MYD88	0.542	ACTR1B	0.539	PHKA2	0.539	AGAP3	0.536	HS6ST1	0.536
ALDH3A2	0.549	ORMDL1	0.549	ZRANB2	0.549	IREB2	0.545	ZNF417	0.545	NBEAL2	0.542	AHDC1	0.539	PKN1	0.539	ALDH16A1	0.536	HSBP1	0.536
ANXA1	0.549	PAIP1	0.549	AARS2	0.545	ITM2B	0.545	ZRANB1	0.545	NDUFA3	0.542	ANAPC1	0.539	PLIN3	0.539	ALOX5	0.536	IFIT5	0.536
ARHGAP24	0.549	PCBP1	0.549	AATF	0.545	KIAA1143	0.545	ACP5	0.542	NMRAL1	0.542	ARL2BP	0.539	POLR1A	0.539	AMD1	0.536	INADL	0.536
ARHGEF7	0.549	PDK1	0.549	ABCC1	0.545	LAMA4	0.545	AHCYL1	0.542	NRBP2	0.542	ATP6V0D1	0.539	PRKCI	0.539	AMFR	0.536	IQCE	0.536
ARL6IP1	0.549	PLCG1	0.549	ACOX3	0.545	LMNB1	0.545	AIMP1	0.542	NSD1	0.542	BMP2K	0.539	PSMG2	0.539	ASCC2	0.536	ITGB5	0.536
ARRDC3	0.549	PNP	0.549	ACTR2	0.545	LONP2	0.545	ALDH1A1	0.542	NUDCD2	0.542	BRD7	0.539	PTMS	0.539	ASXL1	0.536	KLHDC4	0.536
ASL	0.549	POLR2A	0.549	ADRBK2	0.545	LPIN1	0.545	ALS2CL	0.542	OTUD6B	0.542	BZW1	0.539	PTPN9	0.539	ATL3	0.536	LAMA3	0.536
ATHL1	0.549	PPP1R15B	0.549	AES	0.545	LZIC	0.545	ANAPC10	0.542	PAM	0.542	C21orf59	0.539	PUF60	0.539	ATP5A1	0.536	LUM	0.536
ATP2C1	0.549	PRDM4	0.549	ARCN1	0.545	MINK1	0.545	ANKRD40	0.542	PFDN1	0.542	C6orf89	0.539	PUM1	0.539	ATP6V1G1	0.536	MAML3	0.536
AXIN1	0.549	PTPN4	0.549	ARPC2	0.545	MRPL38	0.545	ARPC3	0.542	PFDN4	0.542	CCT8	0.539	RAB11A	0.539	B3GALT6	0.536	MAP1B	0.536
BCAM	0.549	PTPRK	0.549	ATG12	0.545	MRPS15	0.545	ARPP19	0.542	PGAM5	0.542	CDC42EP3	0.539	RAB6A	0.539	BASP1	0.536	MAU2	0.536
BECN1	0.549	R3HDM1	0.549	ATG16L1	0.545	MST4	0.545	ATP5C1	0.542	PHC2	0.542	CYBRD1	0.539	REEP5	0.539	BCR	0.536	MBD4	0.536
BSG	0.549	RBBP4	0.549	ATP8B1	0.545	MTF2	0.545	BAD	0.542	PIKFYVE	0.542	CYP1B1	0.539	REPS1	0.539	BUB3	0.536	MED6	0.536
CCNG1	0.549	RBM17	0.549	BAG1	0.545	NADSYN1	0.545	BNIP3	0.542	PLBD2	0.542	CYP20A1	0.539	RHOA	0.539	C11orf57	0.536	MEST	0.536
CCT2	0.549	RNF6	0.549	C1S	0.545	NFKBIZ	0.545	BPTF	0.542	POFUT1	0.542	DDX6	0.539	RNH1	0.539	CASC4	0.536	METTL13	0.536
CD164	0.549	RPLP1	0.549	C8orf33	0.545	NR1H2	0.545	C10orf118	0.542	PPP2R4	0.542	DENND4B	0.539	RPL18	0.539	CD81	0.536	MLLT6	0.536
CHMP5	0.549	RPS6	0.549	CALM2	0.545	NXF1	0.545	C16orf62	0.542	PRDX2	0.542	DHFR	0.539	RPLP0	0.539	CDC42BPA	0.536	MLX	0.536
CHTF8	0.549	RRP1B	0.549	CBR4	0.545	OAT	0.545	C2orf49	0.542	PRKAB2	0.542	DHX36	0.539	RPPH1	0.539	CENPT	0.536	MRPL11	0.536
CLCN7	0.549	RSPRY1	0.549	CCDC117	0.545	ODC1	0.545	C6orf106	0.542	PSD4	0.542	DLAT	0.539	RPS13	0.539	CFI	0.536	MRPL42	0.536
CLOCK	0.549	S100A11	0.549	CCDC50	0.545	PCNA	0.545	CAMKK2	0.542	RAB3D	0.542	DNAJB9	0.539	RTN3	0.539	CLCN6	0.536	MTX3	0.536
CLPB	0.549	SART1	0.549	CKAP5	0.545	PEBP1	0.545	CASP7	0.542	RBM26	0.542	DNMT3A	0.539	RUNX1	0.539	CLPTM1L	0.536	NARS	0.536
COPZ1	0.549	SBNO1	0.549	COL3A1	0.545	PLEKHM3	0.545	CCNC	0.542	RNF20	0.542	EBNA1BP2	0.539	SEC24C	0.539	CNOT1	0.536	NAT10	0.536

COX4I1	0.549	SDHA	0.549	COPS7A	0.545	PLXDC2	0.545	CDK14	0.542	RPL12	0.542	EMD	0.539	SELT	0.539	COL4A1	0.536	NBR1	0.536
CSAD	0.549	SERPINB6	0.549	COX6A1	0.545	POLK	0.545	CFH	0.542	RPS6KA5	0.542	ENO1	0.539	SF3B5	0.539	COMMD6	0.536	NUP153	0.536
OAZ1	0.536	ABCC5	0.533	RBM4	0.533	CSNK2A2	0.530	PSMG3	0.530	CWF19L2	0.527	RDX	0.527	DR1	0.524	RCN1	0.524	CCAR1	0.520
P4HB	0.536	ACADM	0.533	RNASE1	0.533	CTNNA1	0.530	RAB4A	0.530	DCTN1	0.527	RGS12	0.527	ECE1	0.524	RIMKLB	0.524	CEP120	0.520
PABPC4	0.536	ALDH2	0.533	RNASEH2B	0.533	DHX38	0.530	RNF185	0.530	DDX17	0.527	RNF4	0.527	EIF3L	0.524	RNASEH1	0.524	CIRBP	0.520
PDE6D	0.536	ARAP1	0.533	RNASET2	0.533	DIEXF	0.530	RPL14	0.530	DDX46	0.527	RPL35	0.527	ERN1	0.524	RPL15	0.524	CISH	0.520
PDGFRB	0.536	ARHGAP10	0.533	RNF14	0.533	DTNB	0.530	RPS3A	0.530	DNMBP	0.527	RPL7A	0.527	ETFB	0.524	RPL22	0.524	CNOT6	0.520
PGRMC1	0.536	BRIX1	0.533	RNF168	0.533	DVL3	0.530	RUVBL2	0.530	DNTTIP1	0.527	SDCCAG8	0.527	EVL	0.524	RPL27A	0.524	CROCCP3	0.520
PHLDB1	0.536	C16orf72	0.533	RPAP3	0.533	EIF2B5	0.530	SCD	0.530	EI24	0.527	SEC61B	0.527	FANCC	0.524	RPN1	0.524	CSDE1	0.520
PHTF2	0.536	CC2D1A	0.533	RPL3	0.533	EIF3I	0.530	SDHC	0.530	EIF3K	0.527	SEPP1	0.527	FAR1	0.524	RPS6KA4	0.524	DAD1	0.520
PLXNB2	0.536	CCDC59	0.533	RPL30	0.533	EIF4G3	0.530	SGSM2	0.530	EIF4E	0.527	SLC25A40	0.527	FBXO32	0.524	RPS9	0.524	DAG1	0.520
POLR1B	0.536	CCT4	0.533	SEC11A	0.533	EIF5	0.530	SIPA1L2	0.530	ELAVL1	0.527	SLC6A6	0.527	FH	0.524	RPUSD4	0.524	DCXR	0.520
POM121	0.536	CHKA	0.533	SEMA4C	0.533	EP400	0.530	SNORD97	0.530	FAM136A	0.527	SMARCD2	0.527	GABPA	0.524	SAMD1	0.524	DDX42	0.520
PPIF	0.536	CRLF3	0.533	SETD8	0.533	ERAL1	0.530	STK17A	0.530	FAM96A	0.527	SPTY2D1	0.527	GM2A	0.524	SEC31A	0.524	DIS3	0.520
PPP6C	0.536	CTSD	0.533	SGK1	0.533	EXOC1	0.530	STK36	0.530	FBXO42	0.527	SSBP2	0.527	GOLGA2	0.524	SH3BP2	0.524	DNAH1	0.520
PRCP	0.536	DEF6	0.533	SGPL1	0.533	FAM175B	0.530	STRN3	0.530	FUCA2	0.527	SUB1	0.527	GPR108	0.524	SIN3B	0.524	DYNLT1	0.520
PTBP2	0.536	DHCR24	0.533	SLC1A5	0.533	FOXJ2	0.530	TBC1D1	0.530	GADD45A	0.527	SUGP2	0.527	HAT1	0.524	SLAIN2	0.524	EDF1	0.520
PTPDC1	0.536	DHX32	0.533	SQSTM1	0.533	FXYD5	0.530	TBC1D23	0.530	GOLGA7	0.527	SUMO2	0.527	HCLS1	0.524	SMARCA5	0.524	EIF4G2	0.520
PYGB	0.536	DNAJB1	0.533	SRP68	0.533	GTF2A1	0.530	TFG	0.530	HIF1AN	0.527	TBL1X	0.527	HEATR2	0.524	SREK1IP1	0.524	EPB41L1	0.520
RANBP10	0.536	DNMT1	0.533	SRRM1	0.533	GTPBP4	0.530	TIAL1	0.530	HSPA8	0.527	TMEM184B	0.527	HES1	0.524	SSU72	0.524	FAM32A	0.520
RBM23	0.536	EHD1	0.533	SSB	0.533	HADH	0.530	TJP1	0.530	JMY	0.527	TMTC2	0.527	HIF1A	0.524	TAOK3	0.524	FASTKD1	0.520
RBMX2	0.536	EIF4H	0.533	STARD7	0.533	HADHA	0.530	TK2	0.530	KCTD12	0.527	TOLLIP	0.527	HIGD1A	0.524	TFDP1	0.524	FBXO21	0.520
RINT1	0.536	EPHA4	0.533	STOM	0.533	HBP1	0.530	TMED2	0.530	KDELC2	0.527	TOR1AIP1	0.527	HM13	0.524	TGFB1	0.524	FCER1G	0.520
RNF40	0.536	ETFA	0.533	SUCLG1	0.533	HIST1H2AC	0.530	TMEM219	0.530	KIAA1279	0.527	TSR2	0.527	HTATIP2	0.524	TMC6	0.524	GLB1	0.520
RNF7	0.536	FASN	0.533	TBC1D9B	0.533	IFITM2	0.530	TMEM30A	0.530	KIRREL	0.527	TUBGCP2	0.527	ICK	0.524	TRAF7	0.524	GSTO1	0.520
RPLP2	0.536	FKBP4	0.533	TCF7L2	0.533	ITGAV	0.530	TMEM9	0.530	KLC4	0.527	UBE2N	0.527	IFT46	0.524	TRIM14	0.524	GTF3C3	0.520
RPS15	0.536	G3BP2	0.533	TMEM173	0.533	ITPRIPL2	0.530	TRIT1	0.530	KLHL11	0.527	UBN1	0.527	IFT81	0.524	UBE2G1	0.524	GUSB	0.520
S100A10	0.536	GNG12	0.533	TNKS1BP1	0.533	KPNA4	0.530	UBB	0.530	LAMB2	0.527	UPF1	0.527	IMPDH1	0.524	UGGT1	0.524	HIGD2A	0.520
SAFB2	0.536	GRN	0.533	TPD52L2	0.533	KRCC1	0.530	UBE2E3	0.530	LATS2	0.527	USP8	0.527	IMPDH2	0.524	UHRF2	0.524	HMG20A	0.520
SCARB2	0.536	H3F3B	0.533	TRAK1	0.533	LAMTOR3	0.530	UNC93B1	0.530	LRP1	0.527	UTP14A	0.527	IRF2	0.524	VAMP3	0.524	HPS4	0.520
SEC16A	0.536	HMGN1	0.533	TTN	0.533	LAPTM4B	0.530	USP1	0.530	MRPL20	0.527	WHAMM	0.527	IRF2BPL	0.524	VPRBP	0.524	IBTK	0.520
SEC23B	0.536	HSPG2	0.533	TXNDC11	0.533	LAS1L	0.530	USP47	0.530	MRPL41	0.527	WWP2	0.527	KRT8	0.524	WDR47	0.524	ICMT	0.520
SERPINA1	0.536	IL13RA1	0.533	UBR1	0.533	MAD1L1	0.530	VPS26A	0.530	MXD4	0.527	YWHAQ	0.527	LASP1	0.524	WDR75	0.524	IFI16	0.520
SETD4	0.536	ILVBL	0.533	USP32	0.533	MAN1B1	0.530	VPS26B	0.530	MXRA7	0.527	ZER1	0.527	LDHA	0.524	WDR91	0.524	INF2	0.520
SETD5	0.536	IPO5	0.533	USP46	0.533	MAP4	0.530	VPS36	0.530	MYO10	0.527	ZNF33A	0.527	LGMN	0.524	ZADH2	0.524	IPO7	0.520
SMARCAL1	0.536	KLF11	0.533	VTI1B	0.533	MAP7D1	0.530	WDR45	0.530	MYOF	0.527	ZNF354B	0.527	LRPAP1	0.524	ZNF248	0.524	IVD	0.520
STIM2	0.536	LDLRAP1	0.533	ZNF451	0.533	MCFD2	0.530	WRNIP1	0.530	NCOA4	0.527	ADI1	0.524	MANF	0.524	ZNF280D	0.524	LCOR	0.520
STK38L	0.536	LZTFL1	0.533	ZNF595	0.533	MEAF6	0.530	YAP1	0.530	NDUFV1	0.527	AKAP11	0.524	MCTS1	0.524	ZNF621	0.524	LRRC47	0.520
SUCLA2	0.536	MAEA	0.533	ZNF638	0.533	METTL14	0.530	ZC3H12A	0.530	NFKB2	0.527	AP1B1	0.524	MGST1	0.524	ADAM10	0.520	LUC7L	0.520

SUZ12	0.536	MAPK8IP3	0.533	ABCF2	0.530	MRPL15	0.530	ZNF282	0.530	NRP2	0.527	APEX1	0.524	MID1IP1	0.524	ADCK3	0.520	LY6E	0.520
TIMM13	0.536	MCM6	0.533	ACBD5	0.530	MRPL18	0.530	ZNF333	0.530	NSA2	0.527	APH1A	0.524	NCK1	0.524	ADD3	0.520	MAP1LC3B	0.520
TM2D2	0.536	MID1	0.533	ACP1	0.530	MRPL30	0.530	ABLIM1	0.527	OMA1	0.527	APLP2	0.524	NECAP2	0.524	ADK	0.520	MAP3K2	0.520
TMEM115	0.536	MPHOSPH8	0.533	ALG2	0.530	MRPS18A	0.530	ADH5	0.527	ORC4	0.527	ASPH	0.524	NUDCD1	0.524	AGL	0.520	MFF	0.520
TMEM87B	0.536	MRPL17	0.533	ALMS1	0.530	MRPS23	0.530	AKIRIN1	0.527	OS9	0.527	BAG3	0.524	NUPL1	0.524	AHSA1	0.520	MKNK1	0.520
TNFAIP1	0.536	MRPS14	0.533	ANTXR2	0.530	MSH2	0.530	AP2A2	0.527	P4HA2	0.527	BBX	0.524	OSBPL8	0.524	AKNA	0.520	MRPS7	0.520
TRIM56	0.536	MTX2	0.533	ARHGAP42	0.530	NADK	0.530	AP3D1	0.527	PEF1	0.527	BCL9L	0.524	OSBPL9	0.524	AKR1A1	0.520	MYO1B	0.520
TRIP12	0.536	NFRKB	0.533	ARPC1A	0.530	NDUFV3	0.530	ARHGAP1	0.527	PGRMC2	0.527	C9orf142	0.524	OXA1L	0.524	ANKMY2	0.520	NAA20	0.520
TSC22D4	0.536	NMD3	0.533	BANF1	0.530	NFXL1	0.530	ATP1B1	0.527	PLEKHA5	0.527	CAPG	0.524	PARP1	0.524	ANXA7	0.520	NCSTN	0.520
TTC9C	0.536	NPM1	0.533	BAZ1B	0.530	NONO	0.530	ATP5F1	0.527	PLEKHG1	0.527	CCNL2	0.524	PDE5A	0.524	AP1G1	0.520	NFE2L1	0.520
TXNDC12	0.536	NR2F2	0.533	BCL6	0.530	NOP10	0.530	BMS1	0.527	PLSCR4	0.527	CFDP1	0.524	PHLDA3	0.524	AP1M1	0.520	NSFL1C	0.520
UBXN6	0.536	NUPL2	0.533	BLVRB	0.530	OAS2	0.530	CAPNS1	0.527	PPA1	0.527	CHMP6	0.524	PIM2	0.524	AP1S1	0.520	OGFR	0.520
USP10	0.536	PARN	0.533	C6orf211	0.530	OLA1	0.530	CAT	0.527	PPME1	0.527	CLNS1A	0.524	PRDX6	0.524	AP2S1	0.520	PANX1	0.520
VAV2	0.536	PDDC1	0.533	C6orf62	0.530	P4HA1	0.530	CHD1L	0.527	PPP1R7	0.527	CLU	0.524	PROSC	0.524	APEX2	0.520	PARK7	0.520
WBP5	0.536	PDIA3	0.533	CALCOCO1	0.530	PAG1	0.530	CLASRP	0.527	PRKDC	0.527	CSTB	0.524	PSMA2	0.524	ATP6V0C	0.520	PEAK1	0.520
WHSC1	0.536	PDPK1	0.533	CAPZA2	0.530	PIK3R2	0.530	CLEC2D	0.527	PSAP	0.527	CTBS	0.524	PSMB3	0.524	BLOC1S2	0.520	PHF12	0.520
WWTR1	0.536	PFDN2	0.533	CCDC57	0.530	POFUT2	0.530	CLIP1	0.527	PSPC1	0.527	DBI	0.524	PTPLB	0.524	BRAP	0.520	PLEC	0.520
YLPM1	0.536	PFKM	0.533	CDC25B	0.530	PPP1CA	0.530	CMTM4	0.527	PTCD3	0.527	DCAF17	0.524	PTPN11	0.524	C16orf58	0.520	PLRG1	0.520
ZBTB43	0.536	PHB	0.533	CLPTM1	0.530	PRDX1	0.530	CNDP2	0.527	PTK2	0.527	DDX50	0.524	PTRF	0.524	C19orf10	0.520	PMP22	0.520
ZFR	0.536	PRKAR2A	0.533	COASY	0.530	PRELID1	0.530	COX7B	0.527	RAB5C	0.527	DHX30	0.524	RAP1GAP2	0.524	CAPRIN2	0.520	PNN	0.520
AAGAB	0.533	PSMC2	0.533	CPT1A	0.530	PSMC6	0.530	CTPS2	0.527	RAP2C	0.527	DNAJA2	0.524	RBM42	0.524	CBL	0.520	PPIL1	0.520
PSMA7	0.520	CBWD2	0.517	OTUB1	0.517	AKIRIN2	0.514	MYC	0.514	TBC1D10A	0.514	FSTL1	0.511	SNRPE	0.511	DLG1	0.508	PTMA	0.508
PSMB4	0.520	CCT6A	0.517	PAPSS1	0.517	ALG8	0.514	MYL9	0.514	TBC1D14	0.514	GNG5	0.511	SNX3	0.511	ECH1	0.508	PTTG1IP	0.508
PSMB6	0.520	CD47	0.517	PDHB	0.517	ANKRD27	0.514	MYO15B	0.514	TBC1D2	0.514	GOPC	0.511	SNX4	0.511	EIF3G	0.508	RAC1	0.508
PSMD2	0.520	CEP250	0.517	PHF21A	0.517	ANXA5	0.514	MYO9B	0.514	TBCD	0.514	GTF3C5	0.511	SRP14	0.511	EIF3J	0.508	RBX1	0.508
PSMD8	0.520	CHD9	0.517	PLXND1	0.517	API5	0.514	NCBP2	0.514	TCP11L1	0.514	HMOX1	0.511	SRSF2	0.511	EIF5B	0.508	RCC2	0.508
PSME3	0.520	CLCN3	0.517	PPCS	0.517	APOL6	0.514	NCKAP5L	0.514	TM2D3	0.514	HSP90AA1	0.511	SRSF6	0.511	ELF4	0.508	RCN2	0.508
PTPN18	0.520	COX6B1	0.517	PPM1G	0.517	AQR	0.514	NFAT5	0.514	TMED3	0.514	KHNYN	0.511	SURF4	0.511	EXOC8	0.508	RER1	0.508
PTPN23	0.520	CPSF2	0.517	PPTC7	0.517	ARF5	0.514	NFE2L2	0.514	TOMM40	0.514	KIAA1841	0.511	SYK	0.511	F11R	0.508	RHBDD1	0.508
QARS	0.520	CTNND1	0.517	PRKX	0.517	ARPC1B	0.514	NKTR	0.514	TOP1MT	0.514	LBH	0.511	TADA3	0.511	FAM126B	0.508	RNF34	0.508
RAPH1	0.520	CYFIP1	0.517	PRPF31	0.517	ASXL2	0.514	NOL9	0.514	TRAF3IP1	0.514	LMAN2	0.511	TBC1D4	0.511	FBN1	0.508	RPS21	0.508
RPL23	0.520	DAZAP2	0.517	PSMA1	0.517	BDP1	0.514	NPAT	0.514	TRAM2	0.514	LPAR6	0.511	TIAM1	0.511	FTL	0.508	RPS5	0.508
SAV1	0.520	DBNL	0.517	RAB5B	0.517	C11orf73	0.514	NUMA1	0.514	TRIM2	0.514	LRRC59	0.511	TM7SF3	0.511	FYTTD1	0.508	RSL1D1	0.508
SBDSP1	0.520	DDX1	0.517	RARS2	0.517	CCDC88A	0.514	OSMR	0.514	TRIM8	0.514	LSP1	0.511	TMEM141	0.511	GBE1	0.508	RWDD1	0.508
SCAP	0.520	EIF2S2	0.517	RCL1	0.517	CDK7	0.514	PARD3	0.514	TRIP10	0.514	LTBP2	0.511	TMEM168	0.511	GMFB	0.508	SARNP	0.508
SMAP2	0.520	EIF3H	0.517	RILPL2	0.517	CEBPB	0.514	PCNXL3	0.514	TXN	0.514	MAFF	0.511	TMEM33	0.511	GNL2	0.508	SASH1	0.508
SNRNP70	0.520	EIF3M	0.517	RPF1	0.517	CLASP1	0.514	PDCD11	0.514	TXNDC17	0.514	MAGEF1	0.511	TP53I3	0.511	GPAA1	0.508	SCOC	0.508
SNX12	0.520	EIF4A3	0.517	RPL11	0.517	COG3	0.514	PIP4K2C	0.514	UBA52	0.514	MAGT1	0.511	TRIM33	0.511	GTF2E2	0.508	SERINC3	0.508
SPOPL	0.520	EXOC3	0.517	RPL31	0.517	CXorf38	0.514	PLOD3	0.514	UBE2O	0.514	MCAM	0.511	TRUB1	0.511	GTF3A	0.508	SFT2D2	0.508

SRRM2	0.520	EXT1	0.517	RPN2	0.517	DDX41	0.514	PLXNB1	0.514	UBP1	0.514	MEPCE	0.511	TUBGCP3	0.511	HAUS5	0.508	SIL1	0.508
SSBP1	0.520	FANCL	0.517	RPS20	0.517	DGCR8	0.514	PPDPF	0.514	UBR4	0.514	METTL7A	0.511	ULK3	0.511	HIST1H4E	0.508	SLC20A1	0.508
TEX261	0.520	FARP2	0.517	S100A6	0.517	DGKD	0.514	PPIA	0.514	UXT	0.514	MICAL1	0.511	USP24	0.511	IGFBP5	0.508	SLC40A1	0.508
THBS2	0.520	FBXW2	0.517	SAT1	0.517	DNAJC10	0.514	PPP2R1A	0.514	VCL	0.514	MLEC	0.511	VCP	0.511	INPPL1	0.508	SNRK	0.508
THOC7	0.520	GATAD1	0.517	SBDS	0.517	DPY30	0.514	PPP2R1B	0.514	ZC3H15	0.514	MOGS	0.511	VWF	0.511	JUN	0.508	SNX21	0.508
TIMM17A	0.520	GCN1L1	0.517	SCCPDH	0.517	EIF2AK2	0.514	PRKD3	0.514	ZNF395	0.514	MTOR	0.511	ZEB1	0.511	LDB1	0.508	SPATA13	0.508
TLK1	0.520	GLTP	0.517	SENP6	0.517	ERRFI1	0.514	PTGR1	0.514	ZNF91	0.514	MZF1	0.511	A2M	0.508	LRCH3	0.508	SQRDL	0.508
TMED9	0.520	GNPNAT1	0.517	SERINC1	0.517	FAU	0.514	PTPN13	0.514	ACAD9	0.511	NCKAP1	0.511	ABI2	0.508	MAF	0.508	SRF	0.508
TMTC3	0.520	GSN	0.517	SETD1A	0.517	FOXP4	0.514	PURB	0.514	ADAMTS1	0.511	NENF	0.511	ACOX1	0.508	MCL1	0.508	SRSF3	0.508
TNRC6B	0.520	GSR	0.517	SHFM1	0.517	GALNS	0.514	RBM22	0.514	AHNAK	0.511	NUDT21	0.511	AIP	0.508	MCM9	0.508	SSR3	0.508
TRIM5	0.520	GTF2H3	0.517	SLC16A4	0.517	GDI2	0.514	RBM34	0.514	ANAPC7	0.511	NUP160	0.511	ALDH18A1	0.508	MECOM	0.508	TEAD3	0.508
TXNIP	0.520	HDHD2	0.517	SLC35A3	0.517	GGA2	0.514	RBMS3	0.514	ANXA6	0.511	PEX26	0.511	ANP32B	0.508	MED28	0.508	TLK2	0.508
UBL5	0.520	HNRNPH1	0.517	SMC1A	0.517	GMPS	0.514	REEP3	0.514	APP	0.511	PGM1	0.511	AQP3	0.508	MFGE8	0.508	TMEM183A	0.508
UPF3A	0.520	ID3	0.517	SOAT1	0.517	GPI	0.514	RELA	0.514	ARF1	0.511	PIN1	0.511	ARFIP1	0.508	MFSD1	0.508	TPRG1L	0.508
UQCRQ	0.520	IER2	0.517	SPEN	0.517	GTF2A2	0.514	REXO2	0.514	ATP11B	0.511	POR	0.511	ATP6V1D	0.508	MMADHC	0.508	TPT1	0.508
USMG5	0.520	ILF2	0.517	SPINT2	0.517	GTF3C1	0.514	RFX5	0.514	ATP5H	0.511	PPP1R9B	0.511	ATXN10	0.508	MOV10	0.508	TSPAN17	0.508
USP5	0.520	INSIG2	0.517	SREBF2	0.517	HNRNPF	0.514	RNF11	0.514	BCL7B	0.511	PPP2R2D	0.511	AUP1	0.508	MPG	0.508	TTC31	0.508
VAMP8	0.520	INTS4	0.517	STAMBP	0.517	HSP90AB1	0.514	RNPEP	0.514	BHLHE40	0.511	PRSS23	0.511	BAG4	0.508	MRPL3	0.508	TXNDC9	0.508
WASF2	0.520	KDM4B	0.517	STAT6	0.517	HSPA5	0.514	RPL32	0.514	BTF3	0.511	PSMB2	0.511	BCL10	0.508	MTSS1	0.508	UBAC1	0.508
ZBTB33	0.520	KIDINS220	0.517	STIP1	0.517	IDI1	0.514	RPL5	0.514	C14orf2	0.511	PTPLAD1	0.511	BDH2	0.508	MYO18A	0.508	UQCRFS1	0.508
ZBTB44	0.520	KLF10	0.517	TCF25	0.517	IFT140	0.514	RPL7L1	0.514	CALM1	0.511	PTPN14	0.511	C3	0.508	NDUFB11	0.508	USP40	0.508
ZCCHC17	0.520	LAMP1	0.517	THOC1	0.517	ITGB1	0.514	RPS3	0.514	CAPN2	0.511	PWP1	0.511	CAMK2G	0.508	NSMCE4A	0.508	UXS1	0.508
ZCCHC8	0.520	LAPTM4A	0.517	TMEM109	0.517	ITGB2	0.514	RPS8	0.514	CAV1	0.511	RAB8B	0.511	CAMLG	0.508	NUP155	0.508	WDR43	0.508
ZFAND5	0.520	LGALS1	0.517	TMEM66	0.517	KEAP1	0.514	RRAGA	0.514	CCDC115	0.511	RAD21	0.511	CAPZA1	0.508	OST4	0.508	WDR61	0.508
ZFYVE20	0.520	LIMK1	0.517	TOMM20	0.517	KIAA1671	0.514	RRM2B	0.514	CD44	0.511	RALB	0.511	CASP3	0.508	PCNT	0.508	WIPI1	0.508
ZNF736	0.520	LIN7C	0.517	TOMM34	0.517	KIAA1715	0.514	RUVBL1	0.514	CD59	0.511	RALBP1	0.511	CCDC91	0.508	PCYOX1	0.508	WRN	0.508
ZYX	0.520	LSS	0.517	TOMM70A	0.517	KPNA3	0.514	SERP1	0.514	CMAS	0.511	RAPGEF2	0.511	CCND2	0.508	PDGFRA	0.508	YY1	0.508
ABCE1	0.517	MAN2B1	0.517	TRA2B	0.517	LRP11	0.514	SESN3	0.514	COX18	0.511	RIOK2	0.511	CDC42EP4	0.508	PDIA4	0.508	ZC3H18	0.508
AHCY	0.517	MAPKAPK3	0.517	TTC14	0.517	LSG1	0.514	SIRT7	0.514	COX7C	0.511	RNF19B	0.511	CDK2	0.508	PEX14	0.508	ZMPSTE24	0.508
AK2	0.517	MARCKS	0.517	TXNRD1	0.517	MACF1	0.514	SKA2	0.514	DCAF7	0.511	RNF214	0.511	CIZ1	0.508	PFKL	0.508	ZNF514	0.508
ANKRD17	0.517	MCC	0.517	UFM1	0.517	MBOAT2	0.514	SLC35B1	0.514	DCTN6	0.511	RNF220	0.511	CLTB	0.508	PLD2	0.508	ZNF706	0.508
APTX	0.517	MMS19	0.517	ZBTB1	0.517	MBTPS1	0.514	SLC38A2	0.514	DDX56	0.511	RPL10A	0.511	CNN3	0.508	PNPLA2	0.508	AASS	0.505
ARHGAP32	0.517	MRPL1	0.517	ZBTB4	0.517	MEA1	0.514	SMARCA2	0.514	DERL1	0.511	RPL8	0.511	COBLL1	0.508	POLD4	0.508	ADIPOR1	0.505
ARID5B	0.517	MRPL19	0.517	ZMYM6	0.517	MED4	0.514	SMC3	0.514	DPP9	0.511	RPS12	0.511	COG7	0.508	POLG	0.508	AMPD2	0.505
ASAP3	0.517	MTCH2	0.517	ZNF292	0.517	METTL9	0.514	SND1	0.514	DTX3L	0.511	RRAGB	0.511	CPSF1	0.508	POLR2G	0.508	ATG2A	0.505
BNIP3L	0.517	NAA16	0.517	ZNF317	0.517	MRPL49	0.514	SNRNP27	0.514	DUS1L	0.511	SCRN1	0.511	CSTF1	0.508	PPM1F	0.508	ATG4B	0.505
BROX	0.517	NDUFS8	0.517	ZNF639	0.517	MRPS35	0.514	SPG21	0.514	EEA1	0.511	SDHB	0.511	CTTN	0.508	PPP1CC	0.508	ATP5O	0.505
C9orf3	0.517	NFKBIA	0.517	ZNF655	0.517	MRRF	0.514	SPG7	0.514	EPB41L2	0.511	SLC20A2	0.511	CYB561	0.508	PSMD13	0.508	AURKAIP1	0.505
CABIN1	0.517	NRD1	0.517	AAMP	0.514	MTA1	0.514	STAG1	0.514	FAF1	0.511	SNRPB	0.511	DDX10	0.508	PSMD5	0.508	BCAP31	0.505

CALM3	0.517	OSTF1	0.517	ADCY3	0.514	MTMR6	0.514	TACC3	0.514	FAM134A	0.511	SNRPB2	0.511	DEGS1	0.508	PTGES3	0.508	BFAR	0.505
BTBD2	0.505	EID1	0.505	KIFC3	0.505	PPT1	0.505	TRAP1	0.505	ATP5B	0.502	FAM114A1	0.502	MED13L	0.502	PRPF8	0.502	TMPO	0.502
C19orf66	0.505	EIF2S3	0.505	LARP4	0.505	PRDX3	0.505	TRIB2	0.505	ATP6V1E1	0.502	FKBP2	0.502	MED24	0.502	PRPS2	0.502	TMSB10	0.502
C1orf43	0.505	EIF4EBP2	0.505	LCP1	0.505	PRR13	0.505	TWISTNB	0.505	AXL	0.502	FKBP8	0.502	MGRN1	0.502	PSMA5	0.502	TOB2	0.502
C4orf3	0.505	ENY2	0.505	LSR	0.505	PRRC1	0.505	UBC	0.505	BAG5	0.502	FYB	0.502	MLH1	0.502	PSMC3	0.502	TOM1L2	0.502
C9orf78	0.505	EPN1	0.505	LZTS2	0.505	PTDSS1	0.505	UBE2D2	0.505	BAIAP2	0.502	GALNT1	0.502	MMP24	0.502	RAB34	0.502	TPMT	0.502
CANX	0.505	FAM160B1	0.505	MARK4	0.505	RAB11B	0.505	UBQLN4	0.505	BLCAP	0.502	GDAP2	0.502	MPDZ	0.502	RCBTB1	0.502	TRAF3IP2	0.502
CAPRIN1	0.505	FAM199X	0.505	MCM3	0.505	RBM5	0.505	UBXN1	0.505	BTAF1	0.502	GHITM	0.502	MPHOSPH10	0.502	RHBDF1	0.502	TRIM28	0.502
CAPZB	0.505	FGFR1	0.505	MDFIC	0.505	RFC1	0.505	UGDH	0.505	CALR	0.502	GJA1	0.502	MSN	0.502	RNF169	0.502	TRIOBP	0.502
CCT7	0.505	FN1	0.505	MRE11A	0.505	RIOK3	0.505	UPP1	0.505	CAMSAP1	0.502	GMDS	0.502	MYH11	0.502	RPA2	0.502	TSPAN14	0.502
CNBP	0.505	GALK2	0.505	MREG	0.505	RPS11	0.505	UQCRC2	0.505	CCNK	0.502	GNB2L1	0.502	NANS	0.502	RPL26	0.502	TWF1	0.502
CNP	0.505	GFPT1	0.505	MTDH	0.505	RPS25	0.505	URB1	0.505	CD14	0.502	GPX4	0.502	NDUFA12	0.502	RPS4X	0.502	UBA1	0.502
COL18A1	0.505	GLRX3	0.505	MTSS1L	0.505	SAE1	0.505	VDAC1	0.505	CDC16	0.502	HEG1	0.502	NDUFB3	0.502	RSL24D1	0.502	UBA6	0.502
COX7A2L	0.505	GNAS	0.505	MYL12A	0.505	SBNO2	0.505	VPS25	0.505	CDK4	0.502	HERPUD1	0.502	NDUFB9	0.502	SH3KBP1	0.502	UBE2Q1	0.502
COX8A	0.505	GPX1	0.505	MYO1C	0.505	SCAMP2	0.505	VPS4B	0.505	CEBPZ	0.502	HINT1	0.502	NFIC	0.502	SIAH2	0.502	UQCRC1	0.502
CRTAP	0.505	HADHB	0.505	NAV1	0.505	SDHD	0.505	WDTC1	0.505	CEPT1	0.502	HK1	0.502	NMI	0.502	SLC25A23	0.502	USP31	0.502
CS	0.505	HDGF	0.505	NDUFA10	0.505	SEH1L	0.505	YIPF3	0.505	CHD4	0.502	HNRNPA2B1	0.502	NPTN	0.502	SLC25A46	0.502	USP33	0.502
CTAGE5	0.505	HECA	0.505	NDUFS4	0.505	SLC2A3	0.505	YTHDF1	0.505	CNOT7	0.502	HNRNPK	0.502	NUAK1	0.502	SMAD3	0.502	USP7	0.502
CXorf56	0.505	HEXIM1	0.505	NFIX	0.505	SLC7A1	0.505	ZBTB2	0.505	CRAMP1L	0.502	HSDL1	0.502	NUDC	0.502	SMAD5	0.502	UTP3	0.502
CYCS	0.505	HIST4H4	0.505	NMT1	0.505	SNHG1	0.505	ZNF618	0.505	CTR9	0.502	HSPA9	0.502	OSBPL2	0.502	SNRPC	0.502	WBP11	0.502
CYP51A1	0.505	HSP90B1	0.505	NOP2	0.505	SORBS3	0.505	AASDHPPT	0.502	CUL5	0.502	HSPD1	0.502	PARP6	0.502	SRI	0.502	WDFY1	0.502
DCAF16	0.505	HSPA14	0.505	PABPC1	0.505	SPP1	0.505	ABCF3	0.502	DDOST	0.502	INTS8	0.502	PDCD2	0.502	SSR4	0.502	WDR5	0.502
DCN	0.505	IDH1	0.505	PARVA	0.505	STARD10	0.505	ABHD11	0.502	DENND3	0.502	KAT5	0.502	PDCD4	0.502	STAM2	0.502	WSB2	0.502
DDX5	0.505	IER3IP1	0.505	PEA15	0.505	STRAP	0.505	ACTR1A	0.502	DHPS	0.502	KDELR1	0.502	PDE7A	0.502	STAT2	0.502	ZCRB1	0.502
DPF2	0.505	ISCA1	0.505	PGPEP1	0.505	STX10	0.505	AK3	0.502	DIS3L	0.502	KRTCAP2	0.502	PDLIM1	0.502	SVIL	0.502	ZFYVE27	0.502
DRAP1	0.505	JKAMP	0.505	POLR1D	0.505	TLN1	0.505	ARAF	0.502	DNM1L	0.502	LGALS3BP	0.502	PGK1	0.502	TACC1	0.502	ZMYM1	0.502
DST	0.505	KAT2A	0.505	POMP	0.505	TMBIM6	0.505	ARL5A	0.502	DYNLL1	0.502	LOC100507217	0.502	PIM3	0.502	TBRG4	0.502	ZMYM2	0.502
DUT	0.505	KDM3A	0.505	POP4	0.505	TMEM87A	0.505	ATG13	0.502	EFTUD1	0.502	LOC220729	0.502	PITHD1	0.502	THBS1	0.502	ZNF107	0.502
DYNC1LI2	0.505	KIAA0100	0.505	PPL	0.505	TPM3	0.505	ATG2B	0.502	ESD	0.502	LRRC16A	0.502	POLR2J4	0.502	TMEM106C	0.502	ZNF121	0.502
EBP	0.505	KIAA1598	0.505	PPP4C	0.505	TRAM1	0.505	ATP1A1	0.502	ETS1	0.502	MED12	0.502	PPFIBP1	0.502	TMEM43	0.502		